

CONFIDENTIAL

CONFIDENTIAL

AVGRADERT
Dato: 17.11.09 Sign.: SEi

FFIE

Intern rapport E-253

Reference: 130

Date: January 1976


A LASER GUIDED, SEMIACTIVE MORTAR GRENADE

by

P Bugge-Asperheim

Approved

Kjeller 19 January 1976


Karl Holberg
Superintendent

FORSVARETS FORSKNINGSINSTITUTT
Norwegian Defence Research Establishment
P O Box 25 – N-2007 Kjeller
Norway

CONFIDENTIAL

CONFIDENTIAL

CONFIDENTIAL

CONFIDENTIAL

FFIE

Intern rapport E-253

Reference: 130

Date: January 1976

A LASER GUIDED, SEMIACTIVE MORTAR GRENADE

by

P Bugge-Asperheim

Approved

Kjeller 19 January 1976



Karl Holberg
Superintendent

FORSVARETS FORSKNINGSINSTITUTT
Norwegian Defence Research Establishment
P O Box 25 – N-2007 Kjeller
Norway

CONFIDENTIAL

CONFIDENTIAL

CONTENTS

	Page
1	THE ARMOURED VEHICLE THREAT 5
2	REQUIREMENTS 5
2.1	Grenade parameters 5
2.2	Weapon coverage 6
2.3	Target window 7
2.4	Weapon effectiveness 9
2.5	Laser designator 10
2.6	Homing accuracy 11
2.7	Vulnerability 12
2.8	Electronic countermeasures 12
2.9	Discussion of requirements 13
3	ELEMENTS OF A GUIDED GRENADE 15
3.1	Electro-optic sensors 15
3.2	Aerodynamic surfaces 17
3.3	Guidance principles 20
3.3.1	Pursuit guidance 20
3.3.2	Gravity force, moving target and wind error 22
3.3.3	Proportional navigation 23
3.3.4	Constant bearing 25
3.3.5	Terminal dead reckoning 28
3.3.6	Grenade roll and gravity force revisited 31
3.4	Simulation results 32
3.4.1	On--off control 32
3.4.2	Roll, precession and gravity 32
3.4.3	Moving target 33
4	DESIGN OF A HOMING GRENADE 35
4.1	Functional description 35
4.2	Cost estimate 38
4.3	Project organization 40
5	CONCLUSION 42
	References 42

A LASER GUIDED, SEMIACTIVE MORTAR GRENADE

SUMMARY

The requirements for a laser guided, semiactive mortar grenade to counter an armoured vehicle threat is established. The technical feasibility of such a weapon is investigated. A practical design is described. Development and production costs are estimated.

1 THE ARMoured VEHICLE THREAT

An army attempting to invade Norway is expected to be equipped with a high ratio of armoured vehicles to number of soldiers. The basic attack unit may consist of one tank and three armoured personnel carriers (APC).

The mortar grenade is primarily an antipersonnel weapon. When carried in armoured vehicles, enemy soldiers will not be vulnerable to mortar bombardment, since only direct or close hit will cause damage. With the possibility of a modified grenade with terminal homing, the mortar would regain the traditional role of antipersonnel weapon. The homing grenade would force the infantry away from the armoured vehicles, whereafter conventional grenades would be employed.

The homing grenade would also be effective against tanks. Armoured counterattacks are limited by our small number of tanks. As a complement to direct line of site weapon such as TOW and Carl Gustaf, the indirect or ballistic homing mortar grenade would be a valuable antitank weapon.

The homing sensor might detect infrared heat from the vehicle, or the spot of light from a laser designator pinpointing the target. Only the latter will be discussed in the sequel, since it will have superior probability of direct hit. Equipped with laser, the operator may also designate cool targets such as a stronghold. It is quite conceivable, however, to have alternate grenades with IR sensor for tactical situations when there is no observation post to laser designate the target.

A study to investigate the practical design of a semiactive guided mortar grenade has been conducted at NDRE, in particular by P A B Toombs and J I Ytreeide. This report describes some of the results.

2 REQUIREMENTS

2.1 Grenade parameters

The antipersonnel mortar grenade with fragmenting charge will have no effect on heavy armour.

For three grenades with conical shaped charge the damage probabilities (halt, no more firepower, and/or personnel disabled), provided direct hit, are shown in Table 2.1.

VEHICLE	P_d 81 mm	P_d 107 mm	P_d 120 mm
HEAVY ARMOUR TANK (T54)	0.36	0.46	0.52
LIGHT ARMOUR TANK (PT-76)	0.63	0.74	0.83
ARMoured PERSONELL CARRIER (BTR-50P)	0.32	0.41	0.46
ANTI AIRCRAFT ARTILLERY (ZSU)	0.49	0.57	0.64

Table 2.1 Probability of damage provided hit at 60° impact angle, three calibers with conical shaped charge

Against light APC, shaped charge and fragmenting grenades are probably equally effective (1,2).

The Norwegian Army employs 81 mm and 107 mm mortar grenades. Since the cost of a homing grenade would be 10–100 times that of a regular round without homing, independent of size, only the larger of the two is considered in the following.

A shaped charge requires roll less than 20 rev/s to be effective. The 107 mm grenade is spin stabilized at 100 rev/s during ballistic flight. Therefore, means must be provided to reduce spin to less than 20 rev/s before impact.

2.2 Weapon coverage

One conceivable tactical situation is an armoured attack on Norwegian forces in a valley, as illustrated in Figure 2.1. One battalion will generate a spearhead front line of 2–4 km length. The balance of a brigade will occupy 10 km or more in depth.

The 107 mm mortar has a range of 5.4 km; with a homing head we will assume it to be 4.5 km. If located 2 km behind the main front line, it will cover 2.5 km in depth of enemy territory.

Forward observers with laser designators may be located on the hillsides or in the front line. With a front line of 4 km the required distance from designator on the hillside to a target in the centre of the front could be at least 3 km. The width of a laser beam is typically less than 1 mrad, generating a spot less than 3 m at such range. Field trials in Western Germany (1) indicate target availability 50% at 3 km range due to line of site obstructions, rapidly increasing for shorter range. The maximum range from target to designator is therefore limited by the operator's ability to spot and track the target.

The forward observer may service both the artillery and mortar units. The laser might be the same instrument with one mode for single pulse range measurement and one for continuous designator use.

For comparison, Hotchkiss–Brandt 120 mm towed mortar has a maximum range of 8.1 km with spin stabilized grenades, and 13 km with rocket assisted rounds. The 120 mm light-weight mortar range is 4 km with fin stabilized grenades and 6.5 km with rocket assisted rounds.

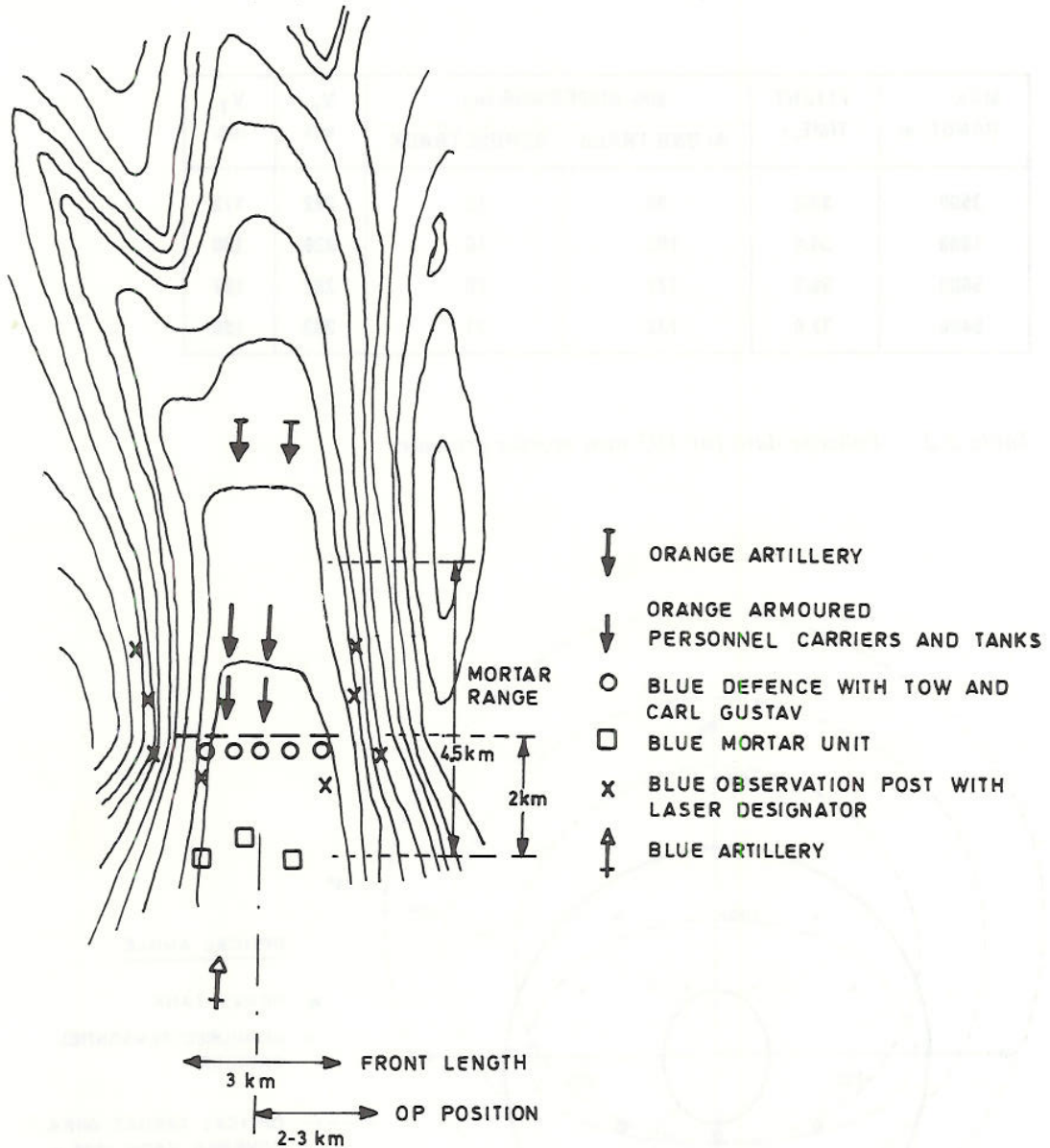


Figure 2.1 A tactical situation

2.3 Target window

The 107 mm grenade is shown in Figure 2.2 Its weight is 12.3 kg. Propulsion charge is 0.326 kg for maximum range 5400 m. Some ballistic data are shown in Table 2.2 (4).

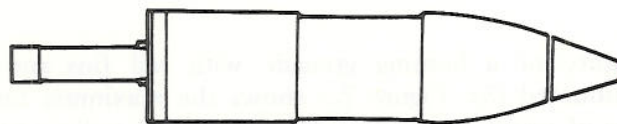


Figure 2.2 107 mm mortar grenade

MAX RANGE, m	FLIGHT TIME, s	50% DISPERSION (m)		V ₀ m/s	V _T m/s
		ALONG TRACK	ACROSS TRACK		
3500	33.2	94	15	222	172
4000	34.4	102	16	239	180
5000	39.1	122	20	282	197
5400	37.0	132	21	293	199

Table 2.2 Ballistic data for 107 mm mortar grenade

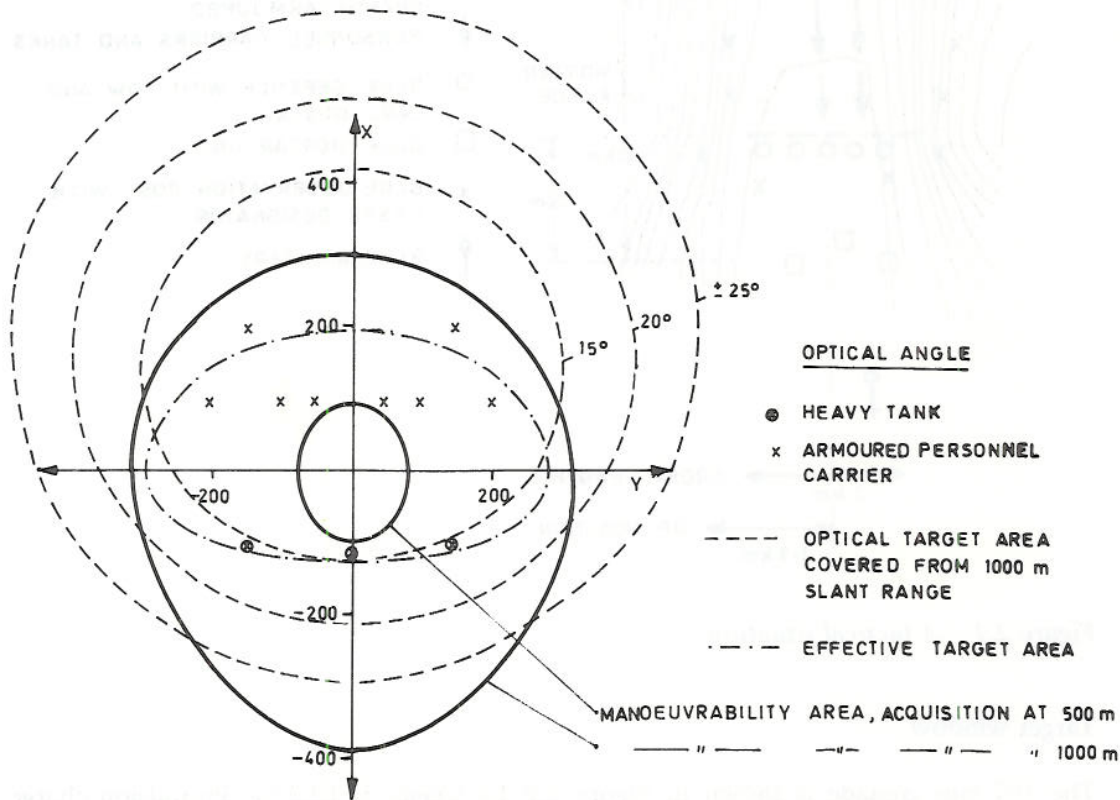


Figure 2.3 Target area and attack unit

A study of manoeuvrability of a homing grenade with tail fins and controllable canard fins has been conducted (5). Figure 2.3 shows the maximum target area for this grenade at two ranges of target acquisition. Plotted as broken lines are the optical coverage at 1000 m range for three different values of optical viewing angle. Only the common area for both manoeuvrability and optical coverage are of interest. Beyond 1000 m the two areas will be increasingly misaligned.

For illustration, assume 4000 m weapon range and $\pm 20^\circ$ optical angle.

At 1000 m acquisition range, effective target area is reduced by the numbers in Table 2.2, assuming other errors negligible. This is shown as a dotted/broken line in Figure 2.3. A typical attack unit of three platoons, each equipped with one heavy tank and three APC, is plotted in Figure 2.3.

1000 m acquisition range is typical for a semiactive unit, 500 m exceeds the practical range for an infrared passive homing grenade by a factor of 2 to 5. Obviously the target area for the latter is insufficient.

2.4 Weapon effectiveness

Let the attack unit of Figure 2.3 advance rapidly at 8 m/s (29 km/h) in mainly open terrain. Assuming prepared target area, time from target position and velocity vector are reported, until launch, may be 25 s. Time of flight from 4000 m is 34.4 s. Hence there is a 60 s delay before the first impact. Time from target acquisition at 1000 m target distance until impact is 7 s. Allow 3 s for change of target. A salvo of 8 rounds at 10 s intervals is launched before realignment of the mortar.

The advance of the tank, the two first APC and the last APC within the target area as a function of time are shown in Figure 2.4. The trajectories are solid lines when illuminated by the designator, otherwise broken lines. The tank is attacked by two rounds, one APC by one and the two others by two rounds each. The eighth round will hit nothing, falling either too far ahead or behind the attack unit.

Let the hit probability be 0.5. The damage probability is calculated in Table 2.3 for each vehicle. Of the 4 vehicles, 1.35 will be damaged. A more moderate advance velocity of 4 m/s and a salvo of 15 rounds would incapacitate 2.25 vehicles.

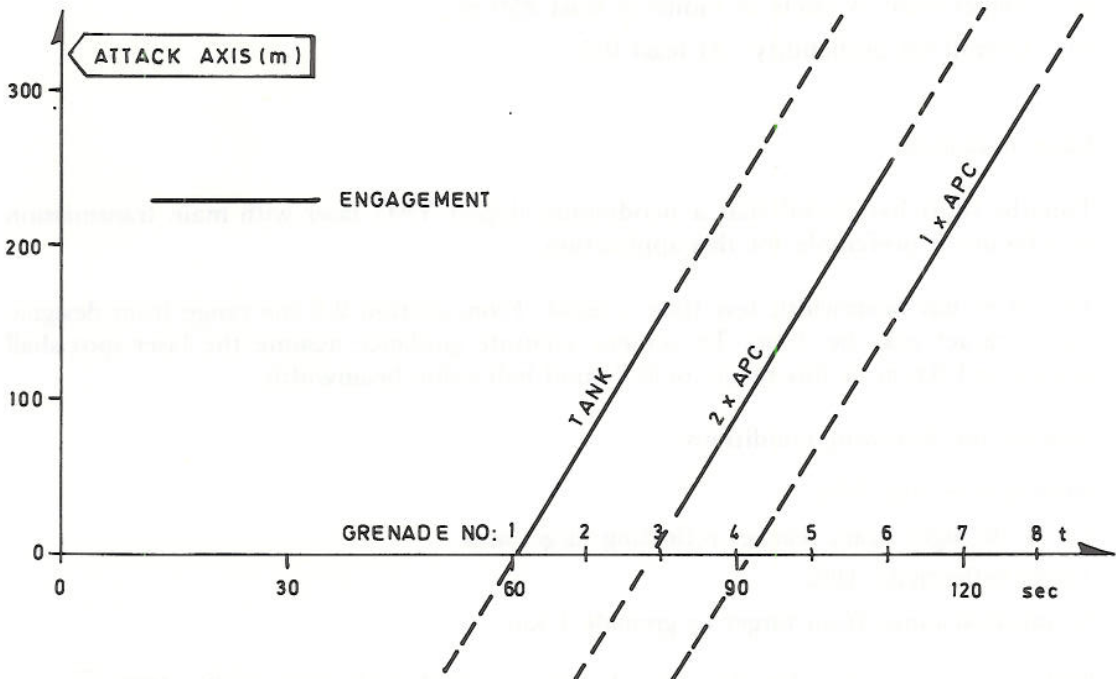


Figure 2.4 Advance of attack unit at 8 m/s

VEHICLE NO	ROUNDS, x		HIT P_t	P_d DAMAGE	SUM DAMAGE	
	8 m/s	4 m/s			$P_s(8\text{ m/s})$	$P_s(4\text{ m/s})$
1 TANK	2	4	0.5	0.46	0.41	0.65
2 APC	2	4	0.5	0.41	0.37	0.60
3 APC	1	3	0.5	0.41	0.20	0.50
4 APC	2	3	0.5	0.41	0.37	0.50
TOTAL NO OF DAMAGED VEHICLES/PLATOON					1.35	2.25

Table 2.3 *Weapon efficiency*

$$\text{Probability of damage: } P_s = 1 - (1 - P_t P_d)^x$$

Though one mortar may cover all three platoons in Figure 2.3, there is not much to be gained since the engagement time for each salvo is limited. It seems reasonable to allocate one mortar and one laser operator to each platoon. An average of 5 incapacitated vehicles of 12 would probably force the enemy to reorganize or wait for reinforcement.

If mutual interference between mortars covering the same target area shall be avoided, coding of grenade and laser signatures is required. Though the laser operator may change code, some operational inconvenience of coding cannot be avoided.

Field trials in rugged terrain in northern Norway (6,7) show that, provided a target is exposed, it is available the required 10 s with probability better than 0.9.

Since the above hypothetical case seems to render a satisfactory weapon efficiency, preliminary design requirements will be stipulated as follows:

- a) Target area: A circle of radius at least 250 m
- b) Overall hit probability: At least 0.5

2.5 Laser designator

Toombs (8,9) has found that a neodymium doped YAG laser with main transmission at $1.06\ \mu\text{m}$ is preferable for this application.

This laser has beamwidth less than 1 mrad. From section 2.2 the range from designator to target may be 3 km. To achieve accurate guidance assume the laser spot shall not exceed 0.6 m at this range, or 0.2 mrad half value beamwidth.

Assume the following conditions:

- Atmospheric loss 50%
- 1% of the light beam reaches reflecting target area
- Target reflectivity 10%
- Acquisition range from target to grenade 1 km

With a suitable seeker for this grenade, the required peak power is $P = 400/\sqrt{\tau}$ watt (9). τ is pulse width in μs . $\tau = 0.1$ renders $P = 1200$ watt.

The sampling theorem requires the pulse rate to exceed twice the information bandwidth. The guidance control bandwidth is approximately 5 Hz. To be able to control or compensate for roll, the pulse rate should be twice the maximum roll rate of 20 Hz (section 2.1). For computational ease in the grenade a pulse rate $f_0 = 100$ Hz is assumed.

A total conversion of $e = 0.12\%$ from battery is conservative. The battery must deliver $E = P \cdot \tau \cdot f_0 / e = 10$ W. A lithium cell of 350 g will supply 10 W for 4 h at -30°C . Hence a portable equipment is quite feasible.

Alignment error between laser and optical aiming device must be the smallest practical value, probably 0.2 mrad. This contributes an error of ± 0.6 m at 3 km range.

The aiming accuracy on a moving target at 3 km under field conditions is assumed to be 0.5 mrad, or ± 1.5 m. Let the aiming error as seen by the seeker when a spot of 0.6 m is illuminating a non-uniform surface on a vehicle be 0.2 m.

Root mean square of these errors is 1.63 m. The portable aiming device is a critical design item.

Preliminary laser designator specifications:

Wave length	1.06 μm
Peak power	1200 W
Pulse length	100 ns
Pulse frequency	100 Hz
Beam width	0.2 mrad
Alignment to optical aiming device	0.2 mrad
Designator weight	20 kg maximum

Pulse coding may be generated with staggered pulse intervals, such as 9:10 and 5:7, or a reference code with certain consecutive pulses missing.

The wavelength of 1.06 μm is infrared and invisible to the eye. An image converter showing an overlay infrared picture in the optical aiming device is feasible. At present it is not considered a requirement.

At low cloud level the laser beam will be stopped at the clouds. No practical increase in peak power will facilitate penetration. With reference to Figure 2.3, a cloud base of 425 m, corresponding to 500 m acquisition range at 60° slant angle, would render a small target area and seriously reduce hit probability against vehicles. Only greatly increased manoeuvrability beyond that which is feasible with conventional canard fins could restore weapon efficiency.

Statistics of cloud base in potential battle fields have not been studied to ascertain whether this is a serious operational handicap.

2.6 Homing accuracy

Computer simulations of the grenade (10) gave several runs with error against stationary targets of 0.3 m or less.

An obvious countermeasure against a guided weapon is to start driving at top speed. A modified control algorithm (11) to home on moving vehicles gives simulation errors less than 0.5 m for 8 m/s. Between 11 and 24 m/s five of ten runs show less than

1.2 m with average of 1.8 m. The dominating error component is along the vehicle velocity vector.

We lack the statistical distribution of vehicle velocity. The simulation runs are few, and the knowledge of how this correlates with a practical system is not firm. Assume a guidance error along the vehicle velocity vector of 1.5 m and 0.4 m across. From section 2.5 expected designator error is 1.63 m at 3 km range. Rms value of both error components renders ± 2.2 m along track and ± 1.7 m across. These errors are within the target area of 6.5×3 m of a typical armoured vehicle. There are also systematic errors, for example a vehicle illuminated from one side will tend to generate an aiming point close to this side of the vehicle. Even assuming that 10% of the grenades will malfunction, an overall hit probability of 0.5, section 2.4, seems to be a conservative value.

Preliminary design requirements on guidance: Hit error shall be less than 1.5 m with target speed from 0 to 20 m/s (72 km/h).

Only conical shaped charge is effective against heavy armour. Light armour such as APC, amphibious tanks and tracked anti aircraft artillery (AAA), however, is vulnerable to fragmenting charge. Extrapolating from (2), the 107 mm fragmented grenade has a kill circle of radius 2.5 m against APC, which would increase somewhat the kill probability for a given distribution in hit error, while also having effect on exposed personnel. Thus the salvo of Figure 2.4 might be 3 rounds with shaped charge, followed by 5 with fragmenting charge.

2.7 Vulnerability

With a grenade detecting radar the enemy may calculate the mortar position from the ballistics, and initiate artillery counterattack. When a homing grenade has acquired a target and started manoeuvring, however, the mortar position can no longer be calculated from the radar signal. Counterattack can be expected 3 minutes after detection. A salvo as proposed in section 2.4 takes 80 s, leaving 1 min 40 s to relocate the mortar squad. Conceivable measures against the mortar radar are warning receiver, electronic jammers and rocket assisted radar homing grenades.

A laser detector on the vehicle (12) will show the azimuth angle to a laser threat within $\pm 2^\circ$. Even so, only the small optical part of the laser designator need be visible, making it a small and difficult target to spot and fire on. The laser illuminates the target only 10 s for each homing grenade. In his own interests the laser operator will appreciate a high grenade hit and destruction probability.

A gunner provided with an image converter capable of detecting the diffracted light from lasers not pointing in his direction, could be a threat to the designator. This possibility has not been investigated.

2.8 Electronic countermeasures

Countermeasures to airborne semiactive laser weapons against stationary targets have been evaluated (13).

Smoke is less effective for a moving vehicle. The driver must see his way. A smoke tube pointing forward and 45° to the side will protect against laser from one side. Alternatively, the smoke tube may be controlled in azimuth and activated by a laser

detector. The grenade will see a line target. An image generating seeker may be able to track the original or stronger end of the line.

A repeater jammer that detects the laser pulse and immediately transmits an identical pulse to illuminate a spot on the ground nearby, is another possible countermeasure (13).

The accepted method to negate active jammers is matched pulse position codes. Since keeping the code secret is not feasible, a particular code is loaded into the weapon and the designator just before launch. While this procedure is simple for an aircraft with guided bomb and designator, it may not be practical with the mortar—designator concept. A few alternative methods will be discussed.

One could use a laser pulse of 20 ns and utilize the inherent delay of minimum 50 ns within the repeater. For a fixed stagger code the laser repeater would track and compensate for the delay. The designator can introduce a random time jitter. The repeater would do the same. The designator can use a long pseudorandom code. The code being known, it is not more difficult for the repeater than for the grenade to decode. An active system would use random jitter, correlate transmitted and received signals and reveal the true target. This is not possible in a semiactive system where transmitter and receiver are not colocated.

Since a portable designator of moderate pulse energy shall be used, it is feasible to generate a false target of equal strength to the true target. For a stationary target with a repeater the grenade seeker probably could not discriminate the true from false target. From a moving vehicle, however, it is thought that the true target would suffer smaller variance in amplitude than the false spot reflected from the ground. Hence an image generating seeker might track the more stable target. The cost—effectiveness of such active countermeasures is questionable, since one repeater can reduce hit probability by at most 50%.

When the designator is inaccurately aimed, spillover may generate false targets on the ground. An image generating seeker should be able to filter out the spillover effect. Tactics such as pointing slightly to the side until 2 s before impact to negate countermeasures (13), may not be effective if a laser detector (12) can trigger on diffracted light from a designator pointing 5–10 mrad off axis. This possibility has not been investigated.

In want of a better understanding of which ECM may be employed on armoured vehicles and the effectiveness of ECCM, preliminary requirements shall call for no ECCM capability.

An image generating seeker with simple algorithms to eliminate false targets shall be an option. Field trials and ECM studies are needed to determine if the added cost to a homing grenade is justified.

2.9 Discussion of requirements

Increased manoeuvrability permits an increase in target area. It will also facilitate operation under lower cloud base. Shorter designation period facilitates higher rate of fire and shorter time for the target to initiate countermeasures. Therefore improved manoeuvrability is a high priority item.

Figure 2.5 illustrates that almost any improvement in target hit accuracy will increase weapon efficiency. The limiting factor will probably be the laser designator. A TOW

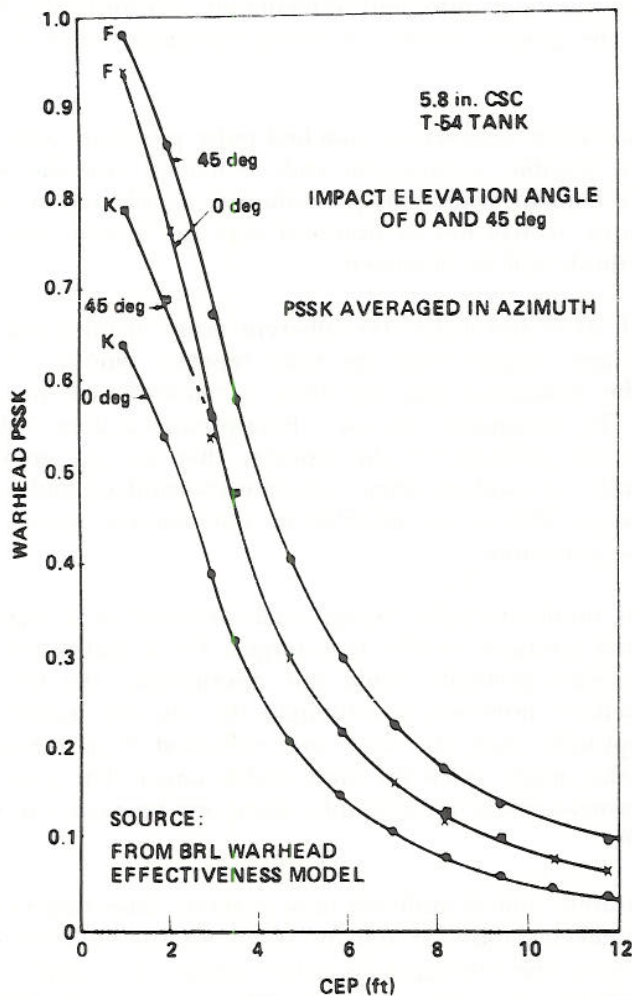


Figure 2.5 Kill probability of a single shot versus delivery accuracy for 5.8 inch grenade with conical shaped charge (14)

0 degrees = horizontal F = fire power kill K = total kill
 PSSK = joint probability of P_k given a hit and probability of hit P_H
 P_H approximately 1 for CEP < 3 ft

designator may have one sigma accuracy of 0.1 mrad (14), or 0.3 m at a distance of 3 km. This is a heavy piece of equipment. A light-weight laser designator suitable for the present purpose is expected to provide less accurate aiming.

Our current understanding of how a homing grenade would be employed favours the lowest possible unit cost. Any improvement that increases production cost must be critically examined, and any possibility of cost reduction should be thoroughly investigated. The preliminary specifications are chosen with the cost factor in mind.

3 ELEMENTS OF A GUIDED GRENADE

3.1 Electro-optic sensors

The commonly used detector for $1.06 \mu\text{m}$ is silicon. An optical bandpass filter of $0.05 \mu\text{m}$ is used to improve signal to noise ratio. From section 2.3 the acquisition angle shall be $\pm 20^\circ$, or preferably $\pm 25^\circ$ to increase target area. Preliminary simulations of the guidance loop call for 0.1° resolution within $\pm 3^\circ$. Three detector configurations have been studied.

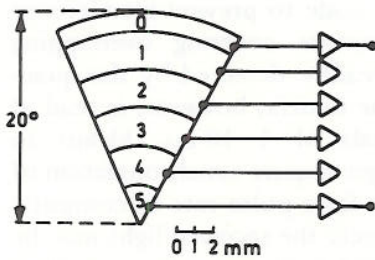


Figure 3.1 Segment detector

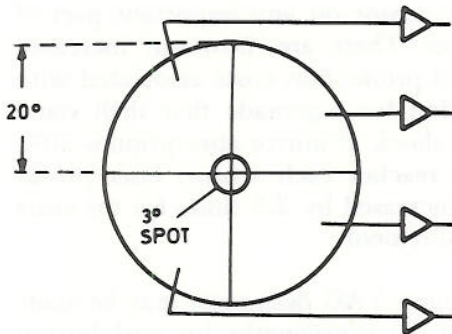


Figure 3.2 Quadrant detector

A rather simple segment detector as shown in Figure 3.1 profits by the grenade spin (9). For each rotation the segment will scan the desired optical solid angle. At least two pulses should be received each time the segment passes through the laser axis. Assume the spin is controlled between 12 and 20 rev/s, and segment angle is $\pi/4$. Then a pulse frequency of 6 kHz is required. The power consumption will increase from 10 W at 100 Hz to 600 W at 6 kHz. A lithium battery of 2 kg is required for 15 min of continuous operation, which is shorter than desirable for a portable designator. Resolution is too coarse for precision terminal guidance (5).

A quadrant detector, Figure 3.2, has been used for similar experiments in the USA (15). By defocusing the spot to 3° and comparing amplitude from the four segments, resolution of 0.1° within $\pm 3^\circ$ from grenade axis is feasible.

Between 3° and 20° only quadrant indication of roll angle to the target is available, which is sufficient for acquisition and coarse correction to within 3° from the grenade axis. A quadrant detector renders simple processing electronics for a single target spot. It would guide the grenade to some weighted middle between a false and a true target. Spots that are not simultaneously illuminated could be resolved by a processor.

A charge coupled matrix detector is image generating and will permit signal processing of several illuminated spots generated by spillover, countermeasures or unwanted secondary reflexes. This detector is read out on a serial pulse amplitude basis, one line at a time. Upper read speed limit is 10^7 elements/s due to noise contributed by the transfer process. With 0.1° resolution and $\pm 20^\circ$ optical angle a 400×400 matrix is required, which is beyond the present state of the art. 100×100 is commercial, with 200×300 on sample basis at high cost.

A hybrid detector with a 64×64 matrix to cover $\pm 3.2^\circ$ at 0.1° resolution in the centre and a quadrant detector to cover 3.2° to 20° is shown in Figure 3.3. Such matrix is readily available (e.g. Photomatrix Ltd, UK) to acceptable quality and cost. Required signal processing is less than for the straight 400×400 matrix. This hybrid sensor has some resemblance to the human eye, wide detection angle with a small centre region of high resolution.

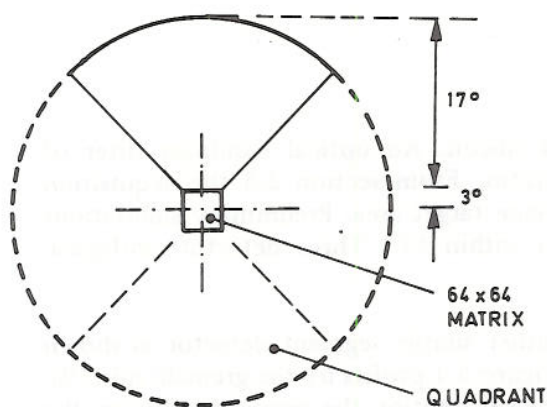


Figure 3.3 Hybrid detector

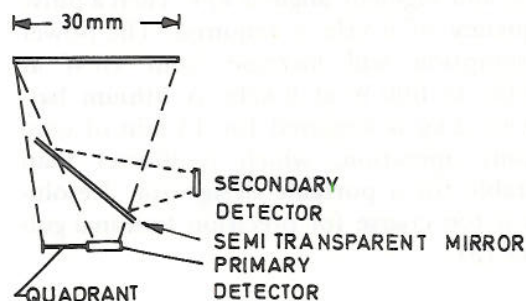


Figure 3.4 Twin detector

0.946	MICROMETER	1
1.0519	"	2
1.0612	"	3
1.0642	"	- LESS THAN 0.01 FROM NO 3
1.0736	"	4
1.1119	"	5
1.1158	"	- LESS THAN 0.01 FROM NO 5
1.1225	"	6
1.338	"	- LESS THAN 0.01 FROM NO 7
1.358	"	7

Table 3.1 Possible wavelengths of Nd-YAG laser

Three of the four quadrants (broken line in Figure 3.3) can be eliminated to render a segment detector. With 100 Hz pulse repetition frequency and spin rate controlled between 12 and 20 Hz, at least one pulse per revolution is detected. 12 Hz sample rate is sufficient to guide a control system of bandwidth 5 Hz from acquisition at 20° to within a window of $\pm 3^\circ$.

A pulse stagger code to prevent interference between designators covering overlapping target area is readily detected by the quadrant sensor. The matrix, however, is read at discrete intervals of 1–10 ms. Means to detect the stagger require synchronization of frame rate with laser pulse rate or computations. Alternatively the received light may be split by a semitransparent mirror with a secondary path toward a solid slab detector covering $\pm 3.2^\circ$, as shown in Figure 3.4. Use of one segment for 20° to 3.2° on the primary detector will avoid shadow from the secondary sensor on any important part of the former. There are, however, increased design and production costs associated with this solution for a grenade that shall stand 10 000 G shock. If mirror absorption is 20%, and 40% reaches each sensor, laser power must be increased by 2.5 times for the same range requirement.

A neodymium YAG designator may be made to lase at 10 wavelengths by push-button control, see Table 3.1.

An optical filter for mass production shall not discriminate wavelengths closer than $0.01 \mu\text{m}$, rendering 7 possibilities. Assume that 3 wavelengths are chosen for A, B and C grenades.

Attenuation of neighbouring wavelength with production tolerances may not exceed 1000, but this is satisfactory to reduce the probability of interference to a small value. The latter method is preferred coding for a matrix detector.

An active jammer can have instant wavelength detection and transmission capability with some increase in complexity.

Consider a seeker using wavelength to negate interference and two matrix sensors, one of which is infrared sensitive. A $1/4 \text{ m}^2$ target area 10°C warmer than the surroundings would be detected at 100–200 m range. The seeker would accept only colocated laser and IR spot for a target vehicle. Countermeasures, such as smoke puffs of

correct IR emission, are conceivable but rather difficult to implement. This strong ECCM can, however, hardly be justified on a small homing grenade.

A study of the optical design of the seeker (9) concludes by recommending a 30 mm Fresnel lens. The optical components will limit the resolution to no better than 0.1° within $\pm 3^\circ$ optical seeker angle.

The present understanding of the system indicates no significant difference in performance of guidance toward a single spot, between a quadrant or matrix sensor. At a cost penalty that may run to +25% per grenade, the single matrix detector will maintain high hit probability with a fair amount of natural (spillover, reflections) and deliberate (smoke, jammer) false targets present in the optical window.

3.2 Aerodynamic surfaces

A spin stabilized guided projectile has been proposed for the Swedish coastal artillery (16,17). For a mortar grenade, however, the required manoeuvrability makes tail fins that carry a major part of the load mandatory (18).

The simulation studies have assumed four rectangular tail fins and four canard fins, Figure 3.5, with data for this modified grenade as shown in Table 3.2. The tail fins are semicircular sheets that are folded around the body before launch. Similar fins are found on the Milan anti-tank missile. Maximum lateral acceleration is 3.3g at 0.6 M speed. This renders the theoretically maximum target area due to manoeuvrability shown as solid curves in Figure 2.3. Stability margin is 0.4 calibre, i.e. centre of lift is 107 mm·0.4 behind centre of gravity.

All fins must be folded within the diameter of 107 mm during launch of a mortar grenade. If allowed to unfold just after launch, there will be a tip-off angle. A value of 5° would give 500 m lateral error at a range of 4000 m (5). Therefore the grenade must be spin stabilized during the major part of the ballistic flight. The fins will be opened by a squib at the first acquisition of a target, whereafter there will be a despin period of approximately 0.33 s from 100 Hz to 20 Hz, or 0.68 s from 100 Hz to 3 Hz.

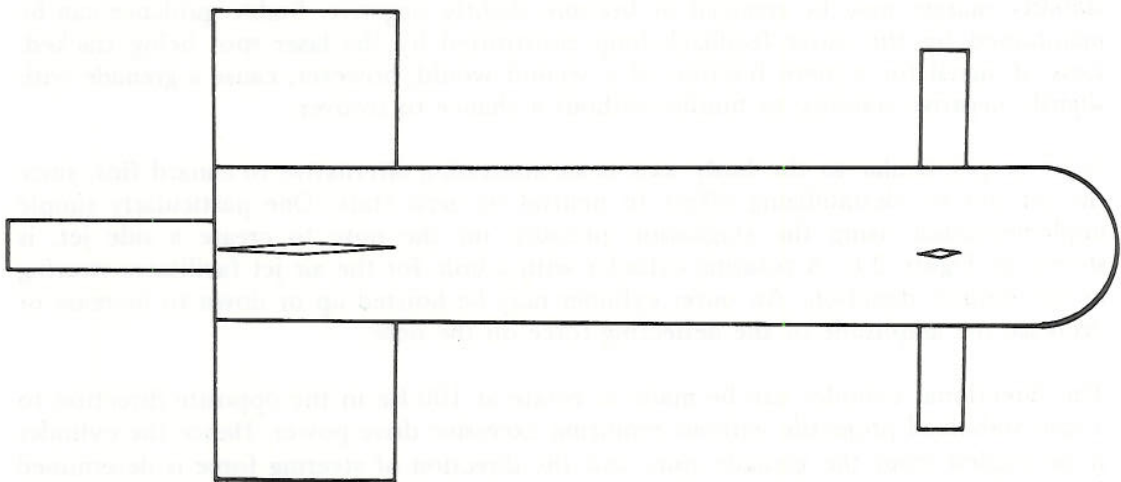


Figure 3.5 107 mm fin stabilized mortar grenade (5) scale 1:5

WEIGHT OF TAIL FINS	1.76 kg
" " CANARD FINS	0.1 kg
" " WARHEAD	3.0 kg
" " BASE PLATE	0.6 kg
" " GUIDANCE SYSTEM	2.5 kg
" " CASING	5.0 kg
TOTAL WEIGHT OF GUIDED GRENADE	13.0 kg
LENGTH	0.64 m
DIAMETER	0.107 m
CENTRE OF GRAVITY MEASURED FROM NOSE	0.35 m
MOMENT OF INERTIA, LONGITUDINAL BODY AXIS	0.025 kg/m²
MOMENT OF INERTIA, NORMAL TO LONGITUDINAL AXIS	0.43 kg/m²
MAXIMUM LAUNCH VELOCITY	270 ms
SPAN, TAIL FINS	30.5 cm
SPAN, CANARDS	24.5 cm
CORD, TAIL FINS	12.0 cm
CORD, CANARDS	3.0 cm

Table 3.2 Data for fin stabilized guided grenade (5)

Larger fin area and/or increase of attainable angle of attack facilitates higher manoeuvrability. However, the tail fin area is limited by what can be unfolded from a cylindrical body in a practical design. Canard fins are destabilizing, since they are mounted forward of centre of gravity. Their surface area, and hence maximum angle of attack, is limited by a certain ratio to the tail fin area for a given stability margin.

Since the canard fins are released after the seeker has acquired the target spot, the stability margin may be reduced or become slightly negative. Stable guidance can be maintained by the outer feedback loop constituted by the laser spot being tracked. Loss of signal for a mere fraction of a second would, however, cause a grenade with slightly negative stability to tumble without a chance to recover.

A jet perpendicular to the body axis is an interesting alternative to canard fins, since the jet has no destabilizing effect in neutral or zero state. One particularly simple implementation using the stagnation pressure on the nose to create a side jet, is shown in Figure 3.6. A rotating cylinder with a hole for the air jet facilitates steering in the desired direction. An outer cylinder may be hoisted up or down to increase or decrease the amplitude of the deflecting force on the nose.

The directional cylinder can be made to rotate at 100 Hz in the opposite direction to a spin stabilized projectile without requiring excessive drive power. Hence the cylinder is decoupled from the grenade spin, and the direction of steering force is determined by the phase angle. By comparison, canard fins are not practical for projectile rotation above 3 Hz because of the unduly high drive power required for rapid change of deflection angle as the fins rotate about the longitudinal body axis.

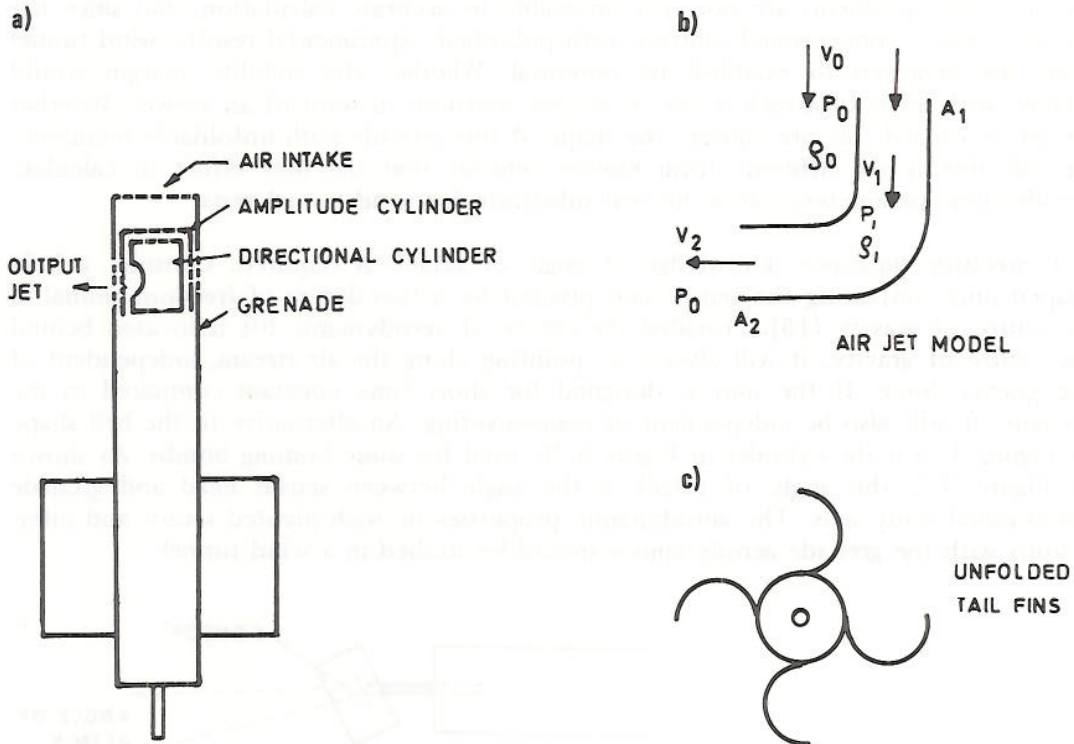


Figure 3.6 Homing grenade with air jet steering (18)

The air jet has no tangential force, and hence cannot roll stabilize the grenade. Rotational speed will depend on the tail fins only. Canard fins may have differential action to control roll. Due to downwash interaction between canards and tail fins and slow response to command, roll stabilization is not considered practical (5). The air jet will obtain correct roll rate and contribute steering force in the desired direction almost immediately after target acquisition and initiation of despin. Information on rotational speed and phase is derived from the electro-optic sensor.

Calculations (18) indicate that the air jet will contribute sufficient steering force, at the penalty of higher drag coefficient, than canard fins. As the inlet is covered with a low drag shield before target acquisition, the increased drag and associated deceleration is suffered only during the last 7 s of flight.

For illustration of the air jet method, consider the simplified model of a rectangular tube of constant cross-section, Figure 3.6b. V_0 is grenade velocity, p_0 and ρ_0 are atmospheric pressure and density, respectively. When the outlet is closed, tube pressure p_1 is by definition equal to stagnation pressure

$$p_s = p_0 + 0.5 \rho_0 V_0^2 = (1 + 0.414) 10^4 \text{ kg/m}^2$$

for $V_0 = 250 \text{ m/s}$ and standard atmosphere. When open, the pressure gradient ($p_1 - p_0$) required to accelerate a quantum of air through the output, must be equivalent to the pressure required to decelerate the same quantum in the inlet tube from V_0 to V_1 . Internal pressure is computed to $p_1 = 1.23 \cdot 10^4 \text{ kg/m}^2$ (18). Let A_1 be input and A_2 be output cross-section area. Output jet force, $F_2 = (p_1 - p_0)A_2$. For $A_1 = A_2 = 60 \text{ cm}^2$, $F_2 = 13.8 \text{ kg}$. The jet steering force coefficient is $C_{NJ} = F_2 / (0.5 \rho_0 V_0^2 A_1) = 0.23 / 0.414 = 0.56$. Another approach (18) renders $C_{NJ} = 0.8$. By comparison, the canard fin steering force is $C_{NC} = 0.6$.

Aerodynamic problems are not very amenable to accurate calculation, and since the air jet is not a conventional solution with published experimental results, wind tunnel trials are required to establish its potential. Whether the stability margin would change with angle of attack is one of several questions in want of an answer. Whether air jet or canard fins are chosen, the shape of this grenade with unfoldable semicircular tail fins is so different from known vehicles that the best effort to calculate aerodynamic parameters can be no real substitute for wind tunnel tests.

For precision guidance, knowledge of angle of attack is required. Consider a bell-shaped unit containing the sensor and pivoted by a two degree of freedom gimbal in its centre of gravity (15). Provided the centre of aerodynamic lift is located behind the centre of gravity, it will always be pointing along the air stream, independent of the gravity force. If the unit is designed for short time constant compared to the grenade, it will also be independent of manoeuvring. An alternative to the bell shape in Figure 3.7a is the cylinder in Figure 3.7b, used for some homing bombs. As shown in Figure 3.7, the angle of attack is the angle between sensor head and grenade longitudinal body axis. The aerodynamic properties of such pivoted sensor and interactions with the grenade aerodynamics should be studied in a wind tunnel.

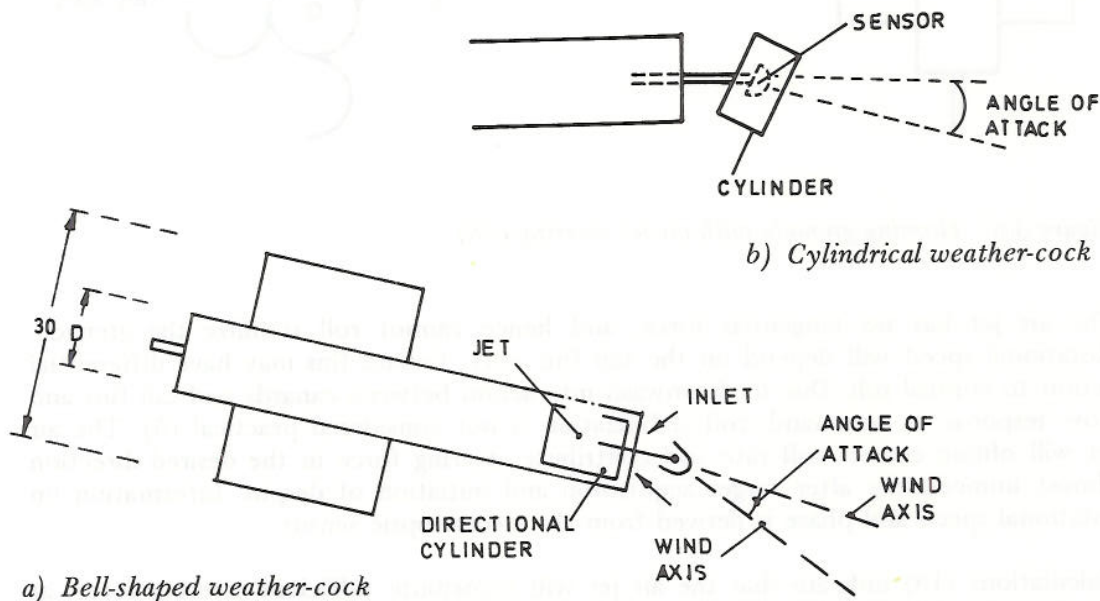


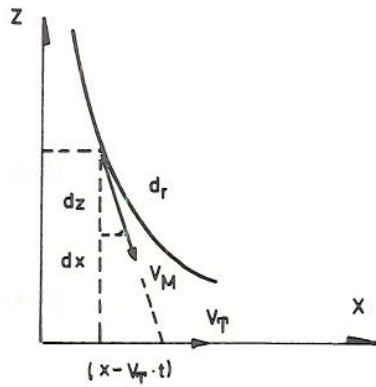
Figure 3.7 Pivoted sensor heads

3.3 Guidance principles

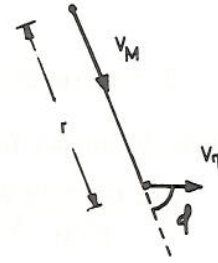
3.3.1 Pursuit guidance

Pure pursuit guidance requires the grenade velocity vector V_M always to point at the target of velocity V_T , Figure 3.8. At time t after the target was at origo $(0,0)$, it is located at $(0, V_T \cdot t)$ and the grenade at (z,x) . The grenade velocity slope will differ from the vertical by

$$\frac{dx}{dz} = \frac{x - V_T \cdot t}{z - 0} \quad \text{or} \quad z \frac{dx}{dz} - x = -V_T t$$



Figur 3.8 Pursuit course



Figur 3.9 Pursuit, polar coordinates

To eliminate t , differentiate with respect to z

$$\frac{d}{dz}(zx' - x) = zx'' = -V_T \frac{dt}{dz}$$

$V_M = dr/dt$, where r is an arc on the trajectory.

$$\frac{dt}{dz} = \frac{dt}{dr} \frac{dr}{dz} = \frac{\sqrt{(dz)^2 + (dx)^2}}{V_M \cdot dz} = \frac{1}{V_M} \sqrt{1 + (x')^2}$$

$$zx'' = (1/p) \sqrt{1 + (x')^2} \quad \text{where } p = V_M/V_T = \text{constant}$$

This non-linear differential equation may be solved (19) for

$$\frac{dx}{dz} = x' = \frac{1}{2} \left[\left(\frac{c_1}{z} \right)^{1/p} - \left(\frac{z}{c_1} \right)^{1/p} \right]$$

$$x = \frac{c_1}{2(1-1/p)} z^{(1-1/p)} - \frac{1}{2(1+1/p)c_1} z^{(1+1/p)} + c_2 \quad (3.1)$$

where c_1 and c_2 are integration constants.

In polar coordinates, Figure 3.9 (20) we obtain for outgoing target

$$\frac{dr}{dt} = \dot{r} = V_T \cos \phi - V_M, \quad r\dot{\phi} = -V_T \sin \phi$$

Dividing

$$\dot{r}/r = (p/\sin \phi - 1/\tan \phi)\dot{\phi} \quad p = V_M/V_T = \text{constant}$$

Integrating

$$r = B (\sin \phi)^{p-1} / (1 + \cos \phi)^p \quad (3.2)$$

where, for initial values r_0 and ϕ_0

$$B = r_0 (1 + \cos \phi_0)^p / (\sin \phi_0)^{p-1}$$

For an incoming target

$$r = B'(1 + \cos \phi)^p / (\sin \phi)^{p+1}$$

where

$$B' = r_0 (\sin \phi)^{p+1} / (1 + \cos \phi_0)^p \quad (3.3)$$

Time of flight to impact for outgoing target

$$t_f = \frac{r(p + \cos \phi_0)}{pV_M - V_T} \quad (3.4)$$

Time of flight to impact for incoming target

$$t_f = \frac{r(p - \cos \phi_0)}{pV_M - V_T} \quad (3.5)$$

Turning rate toward outgoing target

$$\dot{\phi} = -\frac{V_T}{r} \sin \phi = \frac{-V_T(1 + \cos \phi)^p}{B(\sin \phi)^{p-2}} \quad (3.6)$$

Turning rate toward incoming target

$$\dot{\phi} = \frac{V_T}{r} \sin \phi = \frac{V_T(\sin \phi)^{p+2}}{B'(1 + \cos \phi)^p} \quad (3.7)$$

Grenade lateral acceleration

$$a = V_M \cdot \dot{\phi} \quad (3.8)$$

From the above we see that the trajectory of pursuit is a complicated function of $p = V_M/V_T$, whichever coordinate system is chosen. Turning rate and acceleration is bounded for $1 < p \leq 2$, it will go to infinity near impact for $p > 2$. Grenade against vehicle will have $p > 5$, hence it is not possible to maintain pursuit till impact against a moving target.

3.3.2 Gravity force, moving target and wind error

An angle of attack α is required to generate a lift equivalent to the gravity force, Figure 3.10a. $\alpha_g \cong 1^\circ$ for the homing grenade.

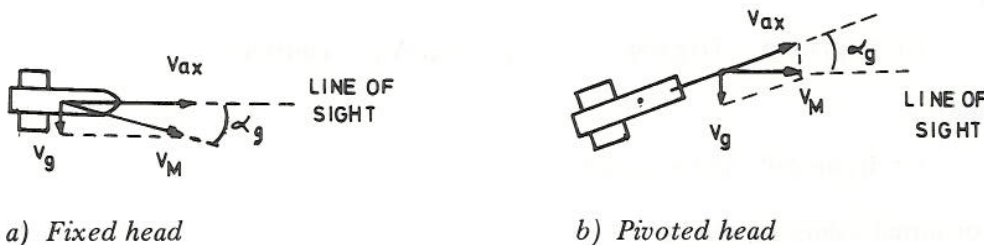


Figure 3.10 Angle of attack due to gravity force

A grenade with fixed seeker and pointing toward the target will have a velocity vector pointing α_g below line of sight to the target, Figure 3.10a. Simulations show an error of approximately 1.3 m at impact for the homing grenade.

A pivoted seeker head (section 3.2) will always point along the air stream. The remaining angle between air stream direction and line of sight to the target is α_g/K , where K is loop gain of the guidance system, see Figure 3.10b. Simulation runs of this configuration against stationary targets show terminal errors of 0.3 m.

As the pivoted seeker will point in the air stream direction, it measures the vector sum of cross wind and target velocity. The grenade cannot discriminate between wind and target velocity.

A missile with pursuit guidance and pivoted head is simulated (21). Having larger wing area, results are applicable to the grenade if multiplied by 1.5. Thus scaled, Figure 3.11 shows terminal errors against a target moving normal to line of sight. Some methods to improve hit capability against moving targets will be discussed in the following.

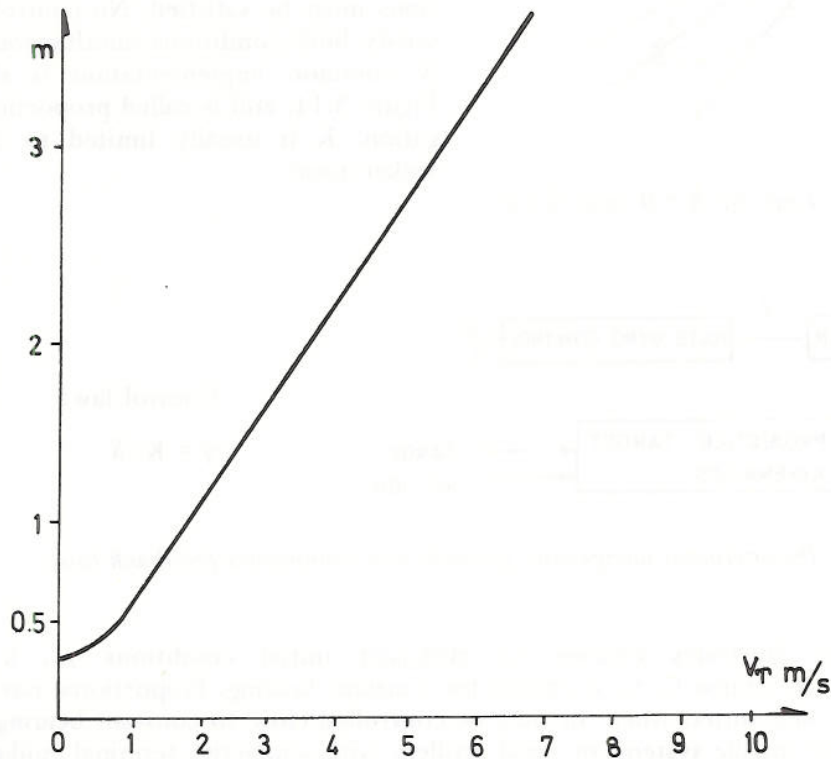


Figure 3.11 Terminal error with target moving normal to line of sight

3.3.3 Proportional navigation

The optimum intercept of a non-maneuvering target is the constant bearing course in which the line of sight from projectile to target is constant in space, Figure 3.12.

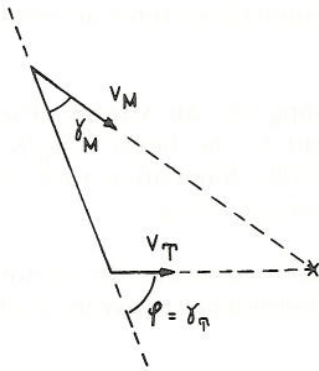


Figure 3.12 Constant bearing course

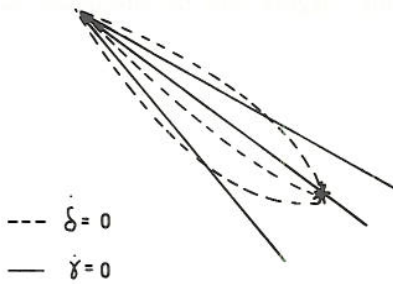


Figure 3.13 Loci of $\delta = 0$ and $\dot{\gamma} = 0$

$$\dot{r} = V_T \cos \gamma_T - V_M \cos \gamma_M$$

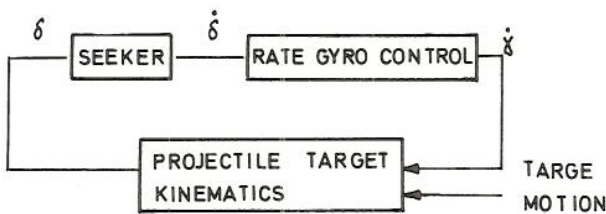
$$r\dot{\phi} = 0 = V_T \sin \gamma_T - V_M \sin \gamma_M$$

From the latter

$$\gamma_M = \arcsin(\sin \gamma_T \cdot V_T / V_M) \quad (3.9)$$

This is the guidance law employed when position and velocity vector of both projectile and target are known, e.g. radar directed anti-aircraft artillery and command guided surface to air missiles.

A semiactive guidance system is lacking distance to the target. However, constant bearing is also characterized by constant projectile-target angle, $\dot{\delta} = 0$, as seen by a grenade with pivoted seeker, and constant projectile bearing in space, $\dot{\gamma} = 0$, as measured by a rate gyro. Figure 3.13 illustrates that both conditions must be satisfied. No control law can satisfy both conditions simultaneously (22). A common implementation is shown in Figure 3.14, and is called proportional navigation. K is usually limited to 5 due to seeker noise.



Control law:

$$\dot{\gamma} = K \cdot \delta \quad (3.10)$$

Figure 3.14 Proportional navigation, grenade and kinematics feedback loop

Figure 3.15 illustrates courses for different initial conditions γ_0 , $k = 2$ and $V_M / V_T = 2$. In course C, γ_0 is chosen for constant bearing. Proportional navigation is particularly well suited when γ_0 may be controlled close to constant bearing, such as surface to air missile systems or naval artillery with semiactive terminal guidance. It is less attractive for the homing grenade where γ_0 cannot be controlled easily. The added cost of a rate gyro is undesirable.

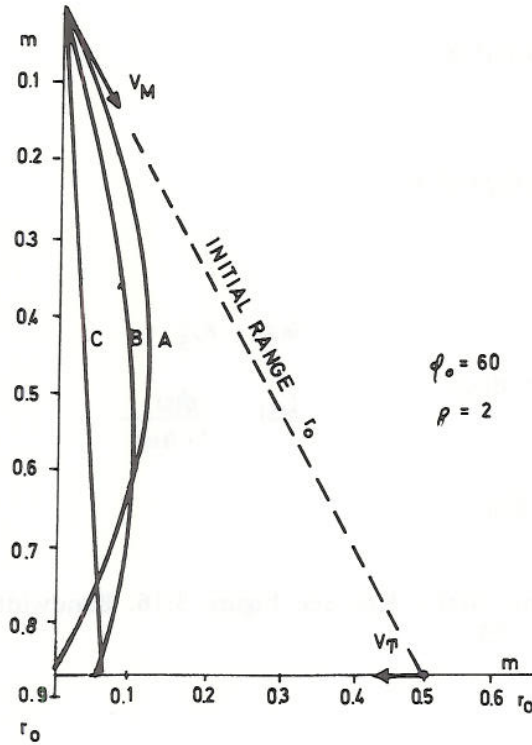


Figure 3.15 Proportional navigation courses (20)

3.3.4 Constant bearing

Pursuit guidance toward a moving target is assumed. At a certain instant, arbitrarily $t = 0$, the required lead angle for constant bearing, $\gamma_M = \arcsin(\sin \gamma_T \cdot V_T/V_M)$, shall be computed from the laser spot and added to the grenade control signal, see Figure 3.12, $\gamma_T = \phi(t = 0)$.

$\phi(t)$ is the driving function to the grenade control system. From section 3.3.1

$$\dot{\phi} = -(V_T/r)\sin \phi = \frac{-V_T (1 + \cos \phi)^P}{B (\sin \phi)^{P-2}} \quad (3.6)$$

$$B = \gamma_0 (1 + \cos \phi_0)^P / (\sin \phi_0)^{P-1} \quad (3.2)$$

$$\begin{aligned} \ddot{\phi} &= \frac{d\dot{\phi}}{dt} = \frac{d(\dot{\phi})}{d\phi} \cdot \frac{d\phi}{dt} = \dot{\phi} \cdot \frac{d}{d\phi} \left[\frac{-V_T (1 + \cos \phi)^P}{B (\sin \phi)^{P-2}} \right] \\ &= -\dot{\phi} \left[\frac{V_T}{B} \sin \phi \cdot p + \dot{\phi} (p-2) (\cotg \phi)^{p-2} \right] \end{aligned}$$

$$\ddot{\phi} = \frac{V_T^2}{r^2} \frac{V_M}{V_T} \sin \phi \left[\frac{\sin^2 \phi}{1 + \cos \phi} + \frac{p-2}{p} \cos \phi \right]$$

For grenade against vehicle, $p = V_M/V_T \gg 1$, $(p-2)/p \cong 1$ and the expression within brackets approaches 1. Hence

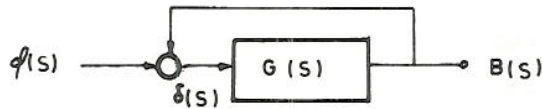
$$\ddot{\phi} = (V_T V_M/r^2) \sin \phi$$

MacLaurin serie

$$\phi(t) = \phi(0) + \dot{\phi}(0)t + \ddot{\phi}(0)t^2/2 \dots$$

Laplace transform

$$\phi(s) = \phi(0) + \dot{\phi}(0)/s + \ddot{\phi}(0)/4s^2 + \dots$$



$$G(s) = K/s$$

$$\delta(s) = \frac{\phi(s)}{1 + G(s)}$$

Figure 3.16 Calculate error function $\delta(s)$

Assume a first order control system, $G(s) = K/s$, see Figure 3.16. Bandwidth 4 Hz, hence: $1 = K/|j2\pi 4|$, $K = 8\pi = 25$.

Error function

$$\delta(s) = (C_0 + C_1s + C_2s^2 + C_3s^3 + \dots) \phi(s)$$

describes the grenade seeker signal components due to zero, first, second etc time derivative of a smoothly changing driving function $\phi(t)$.

How to calculate C_n coefficients is shown in (23). The feedback system of Figure 3.16 has $C_0 = 0$, $C_1 = -1/K$, $C_2 = 1/K^2$, $C_3 = -1/K^3$

$$\delta(s) = \delta_0 + \delta_1 + \dots f_e(s) = 0 \cdot \phi(0) + C_1 \dot{\phi}(0) + C_2 \ddot{\phi}(0)/4 + \dots$$

$$\delta_0 = C_0 \cdot \phi = 0$$

$$\delta_1 = C_1 \cdot \dot{\phi} = (V_T \sin \phi)/(K \cdot r)$$

$$\delta_2 = C_2 \cdot \ddot{\phi} = (V_T V_M \sin \phi)/(4K^2 \cdot r^2) = \delta_1 \cdot V_M/(4K \cdot r)$$

δ_2 is negligible when $\delta_2/\delta_1 = V_M/4K \cdot r_1 < 0.1$.

Let grenade velocity $V_M = 150$ m/s. $r_1 > 10 \cdot 150/4 \cdot 25 = 15$ m.

Hence for

$$r > 15 \text{ m}$$

$$\delta \cong \delta_1 = C_1 \cdot \dot{\phi} \tag{3.11}$$

$$V_T = \delta \cdot K \cdot r / \sin \phi$$

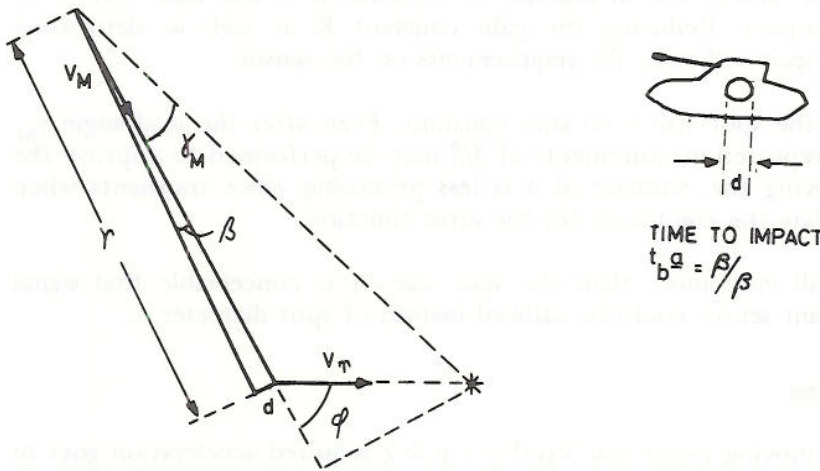


Figure 3.17 Calculate time to impact from laser spot on the target

The solid angle of the laser spot on the target as seen from the seeker (Figure 3.17) is

$$\begin{aligned} \beta &= d/r \\ \dot{\beta} &= d\beta/dt = -\frac{d}{r} \cdot \frac{\dot{r}}{r} + \beta(V_M - V_T \cos \phi)/r = \beta \frac{V_M}{r} (1 - p^{-1} \cos \phi) \\ V_M &= (\dot{\beta}/\beta) r(1 - p^{-1} \cos \phi) \end{aligned} \tag{3.12}$$

Note that time to impact

$$t_b = r/(V_M \cos \gamma_M - V_T \cos \phi) \cong r/\dot{r} = \beta/\dot{\beta} \quad \text{for small } \gamma_M$$

Insert equations (3.11) and (3.12) in equation (3.9) to render the lead angle

$$\gamma_M = \arcsin(\sin \gamma_T \cdot V_T/V_M) = \arcsin[K \cdot \delta(\beta/\dot{\beta}) \cdot (1 - p^{-1} \cos \gamma_T)] \tag{3.13}$$

$\phi = \gamma_T$ at instant of setting γ_M into the control loop and shall ideally remain constant until impact. K is a gain constant, δ, β and $\dot{\beta}$ shall be estimated from the seeker input. $(1 - p^{-1} \cos \gamma_T)$ cannot be estimated without ground reference. For grenade on vehicle $p = V_M/V_T > 10$ will be true for target speed up to 54 km/h. $(p^{-1} \cos \gamma_T) < 0.1$ and may be neglected, $\sin \gamma_M \cong \gamma_M$. Hence we shall use (24):

Lead angle

$$\gamma_M = K \cdot \delta \cdot \beta/\dot{\beta} \tag{3.14}$$

A comment on measurement and resolution for the variables δ and β is in order.

Assume a 64×64 matrix sensor to cover a central area of $\pm 5^\circ$. Resolution $a_1 = 10/64 = 0.16^\circ = 2.73$ mrad. Let $V_M = 150$ m/s, $V_T \sin \phi = 12$ m/s = 43 km/h. Laser spot size $d_1 = 1$ m.

Maximum range to detect target movement: $r_m = V_T/(K \cdot a_1) = 12/25 \cdot 0.00273 = 176$ m. Maximum range at which the laser spot covers two elements: $r_s = d_1/a_1 = 366$ m.

The lead angle to be computed is $\gamma_M = 12/150 \text{ rad} = 4.6^\circ$, which is barely within coverage of this sensor, and it will in practice be introduced at less than 150 m, or one second, before impact. Reducing the gain constant K as well as defocusing (magnifying) the laser spot will relax the requirements on the sensor.

This method requires the spot size d to stay constant. Even after the lead angle γ_M has been introduced, repeated measurements of β/β may be performed to improve the estimate of γ_M . Improving the estimate of δ is less promising, since transients when introducing γ_M invalidate the conditions for the error function.

Though reflectivity will vary more than the spot size, it is conceivable that signal strength from a quadrant sensor could be utilized instead of spot diameter d .

3.3.5 Terminal dead reckoning

For pursuit toward a moving target and $V_M/V_T = p > 2$ required acceleration goes to infinity before impact. Applying more acceleration earlier would prevent the grenade falling behind the target. A method to estimate the instant at which fixed or full acceleration shall be applied (11) will be analysed.

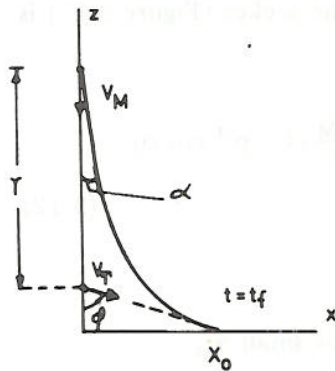


Figure 3.18 Terminal dead reckoning

From section 3.3.1, equations (3.6) and (3.8):

pursuit acceleration

$$a = V_M \dot{\phi} = -\frac{V_M V_T}{r} \sin \phi$$

$$r = -\frac{V_T V_M}{a} \sin \phi$$

pursuit time to impact from equation (3.4)

$$t_f = \frac{r(p + \cos \phi)}{pV_M - V_T} = -\frac{V_T V_M \sin \phi (V_M + V_T \cos \phi)}{a (V_M^2 - V_T^2)} \quad (3.15)$$

A modified course with fixed acceleration a_m introduced at the same position (r, ϕ) has time to impact t_m . For $V_M > 10 V_T$ very nearly $t_m = t_f$.

Grenade ground reference angle is α , and $\alpha_0(t=0) = 0$ (see Figure 3.18).

Since $a_m = V_M \dot{\phi}$ and $\dot{\alpha} = \dot{\phi} = a_m/V_M = c$, then $\alpha = ct + \alpha_0 = ct$.

Grenade lateral displacement with $(\alpha = ct)$ is

$$x_m = \int_0^{t=t_m} a_m (\cos ct) \cdot t \, dt = a_m c^{-2} (\cos ct + ct \cdot \sin ct) + D$$

$$x_m = 0 \text{ at } t = 0, \quad \text{hence } D = -a_m c^{-2}$$

By trigonometric expansion

$$x_m = \frac{1}{2} a_m t_m^2 (1 - c^2 t^2/3) = \frac{1}{2} a_m t_m^2 (1 - e_1)$$

For intercept of non-maneuvering target and $t_m = t_f$

$$t_f \cdot V_T \sin \phi = x_m = \frac{1}{2} a_m t_m^2 (1 - e_1)$$

$$a_m = 2V_T \cdot \sin \phi / [t_f(1 - e_1)]$$

Insert for t_f from equation (3.15)

$$a_m = 2 a \frac{(V_M^2 - V_T^2)}{(V_M^2 + V_M V_T \cos \phi) (1 - e_1)} = 2 a \frac{(1 - p^{-2})}{(1 + p^{-1} \cos \phi) (1 - e_1)} \quad (3.16)$$

ϕ , p and $e_1(a_m, V_T, t_m)$ are not available in the grenade.

Numerical example with worst case values from section 2.6:

$$\phi = 60^\circ, \quad V_M = 150 \text{ m/s}, \quad V_T = 20 \text{ m/s} = 72 \text{ km/h}$$

Approximately

$$t_m \cdot V_T \cdot \sin \phi = x_m \cong \frac{1}{2} a_m t_m^2$$

Then

$$a_m = 2 V_T \sin \phi / t_m$$

$$e_1 = (c t_m)^2 / 3 = (a_m V_M^{-1} t_m)^2 / 3 = p^{-2} (2 \sin 60^\circ)^2 / 3 = p^{-2}$$

Inserting in equation (3.16)

$$a_m = 2 a \cdot 0.98 / (1.0667 \cdot 0.98) = 2 a \cdot 0.94 \quad (3.16a)$$

For

$$V_T = 10 \text{ m/s} = 36 \text{ km/h}, \quad a_m = 2 a \cdot 0.97$$

Hence our estimate of a_m will be equal to or less than 6% in error if we take

$$a_m = 2 a \quad (3.17)$$

From equation (3.11) the pursuit seeker signal, $\delta = C_1 \cdot \dot{\phi} = -\dot{\phi}/K$

$$\text{Acceleration} \quad a = V_M \cdot \ddot{\phi} = V_M \cdot K \cdot \delta$$

V_M is not measured in the grenade, but stays approximately constant during the last path to the target (18). K is control gain. Only $(V_M \cdot K) = \text{constant}$, not its value, is required. At a specific value of $\delta(t=t_m) = \delta_m$, the present actuator input value is doubled, or through non-linear look-up table to the equivalent of $2 \cdot a$, and stays fixed until impact.

Numerical example

$$V_M = 150 \text{ m/s}, \quad V_T = 20 \text{ m/s}, \quad \phi = 60^\circ, \quad t_m = 1 \text{ s}$$

$$t_m \cdot V_T \cos \phi = 10 \text{ m} = x_m = \frac{1}{2} a_m t_m^2$$

then

$$a_m = 20.1 \text{ m/s}^2 = 2.05 \text{ g}$$

6% error due to the inability to differentiate this case from $V_T = 10 \text{ m/s}$, $\phi = 0$ results in error of $x_m \cdot 0.06 = 0.6 \text{ m}$ overshoot.

The value of $a = a_m/2 = 10.05 \text{ m/s}^2$ is a direct function of seeker angle δ . At $t = t_m$ range to target is $r = V_M \cdot t_m = 150.1$ meter. Assume gain constant $K = 25$ as before. We have from equation (3.11): $\delta = V_T \sin \phi / K \cdot r = 0.26^\circ$. With a seeker of resolution 0.16° , this is clearly not sufficient resolution. Reduce K by factor 10. Now seeker resolution is $100 \cdot 0.16 / 2.6 = 7.5\%$ and may contribute an error of 0.75 meters.

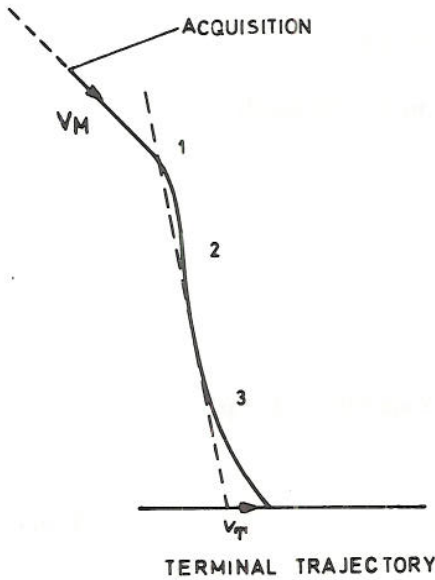


Figure 3.19 Terminal trajectory

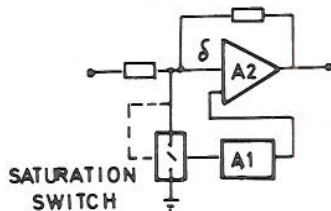


Figure 3.20 Operational amplifier equivalence

Hence worst case error for this example is $x_e = 0.6 + 0.75 = 1.35$ meters.

A low gain will cause deviation from the true pursuit course, which invalidates the above formulas for correction toward a moving target. The grenade is brought back to the pursuit course by an algorithm that is activated when the preliminary transient is completed, point 1 in Figure 3.19. It measures the stationary deviation and introduces an equivalent correction, point 2 in Figure 3.19. This algorithm has slow response, such that the error function is measurable when the angular deviation due to a moving target becomes appreciable, point 3 in Figure 3.19. The equivalent to this function is the very low bandwidth chopper amplifier A1 of an operational amplifier A2 of low gain, Figure 3.20. This algorithm has been tried successfully on the fixed acceleration method (11), and should be equally applicable to the lead angle computation.

The fixed acceleration method utilizes less than the centre $\pm 3^\circ$ for estimation and control. Therefore a simple quadrant detector with the associated simple signal processing is assumed sufficient for this method of guidance.

The estimate of lead angle

$$\gamma_M = K \cdot \delta (\beta / \dot{\beta}) (1 - p^{-1} \cos \phi) \tag{3.13}$$

and fixed acceleration

$$a_m \cong 2a(1 - p^{-2})(1 - e_1)^{-1} \cdot (1 + p^{-1} \cos \phi)^{-1} \tag{3.16}$$

shows almost identical sensitivity to the unknown parameters ϕ and p . Since $a = V_M \cdot K \cdot \delta$, γ_M and a_m also show identical sensitivity to the input signal δ .

Comparing with the lead angle method, fixed acceleration terminal error is a direct function of error in δ , while the former suffers hit error due to inaccurate lead angle γ_M .

The fixed acceleration method suffers a hit error equal to the difference between target position estimated from $t=0$ and real position at $t=t_f$ due to target manoeuvring, while the former is only sensitive to change in target speed. Being under closed loop control to impact, the lead angle method is sensitive to under-damped transients when the lead angle is introduced. It is sensitive to change in spot diameter during the last 2 s of flight, and probably requires a matrix detector. Estimate of time to impact permits time-varying gain K as required in optimal control theory (21).

For illustration, Figure 3.21 shows acceleration of true pursuit, fixed acceleration, and lead angle method. Only the pursuit curve is a result of calculation.

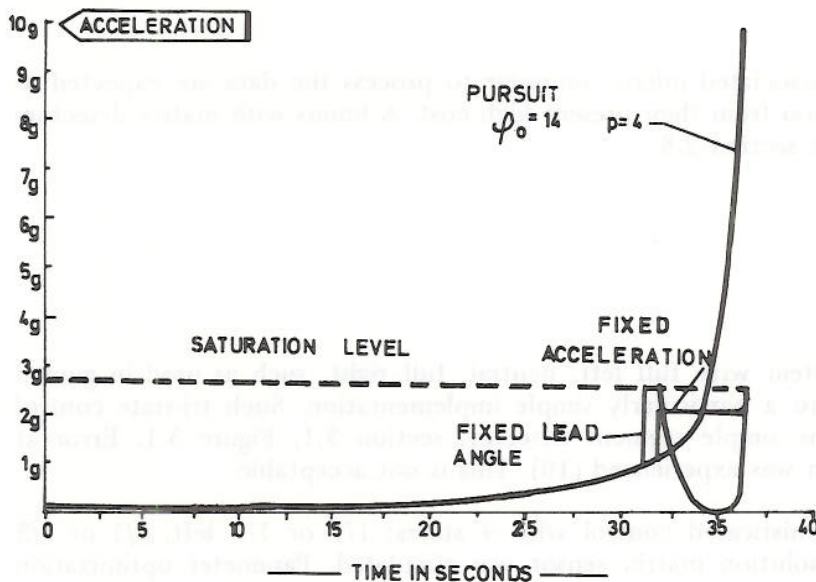


Figure 3.21 Acceleration for three methods of terminal guidance

3.3.6 Grenade roll and gravity force revisited

With a pivoted seeker head the angle between the seeker axis and grenade axis is a good measure of grenade roll angle. With a fixed seeker head the roll angle relative to line of sight to the target is observable by the seeker sensor, except when the target is brought to the roll axis. The spot may be shaped elliptically by an appropriate lens. Thus roll angle to the target is always observable.

Provided the actuators can compensate for the rotation, there is no need to roll stabilize the grenade. Canard fins can compensate for roll not exceeding 3 Hz, while jet steering with rotating cylinder may counter rotate up to 100 Hz. There is a question of circular linearity of the quadrant detector to be investigated experimentally (11). The penalty of roll stabilizing along the air stream axis of the seeker is slow reaction to lateral corrections since the grenade body shall have to yaw like an aeroplane.

The possibility of estimating the required angle of attack to compensate for gravity from the applied actuator input has been proposed (21). The angle of attack is a quadratic function of velocity V_M which is not measured and varies with launch conditions. After a fixed acceleration toward a moving target is initiated, only the

gravity roll angle relative to target angle is remembered. A manoeuvring target will cause gravity compensation that differs from vertical direction. Furthermore, a monotonic error signal (not underdamped oscillations) is desired to prevent confusion of 180° .

If further work shows estimation of angle of attack to be satisfactory, the pivoted head can be substituted for a fixed head. The sensor must have a comparable increase in angle of high resolution of typically $\pm 1^\circ$. This will add $\pm 1^\circ$ to the seeker angle δ_m required to determine instant of initiating fixed acceleration. Linear area of $\pm 3^\circ$ with high resolution is sufficient and believed realizable with a quadrant detector. Constant bearing navigation may require $\pm 5^\circ$ lead angle during the final course. Adding 1° for a fixed seeker head renders $\pm 6^\circ$ with resolution of 0.1° which is thought to be too large for a quadrant detector. Hence a matrix detector of 128×128 elements is needed for the latter method.

Matrix detectors and associated micro computer to process the data are expected to show continual reduction from their present high cost. A bonus with matrix detectors is ECCM capability, see section 2.8.

3.4 Simulation results

3.4.1 On-off control

A tri-state control system with full left, neutral, full right, such as used in guided bombs, usually leads to a particularly simple implementation. Such tri-state control was simulated with the simple segment detector, section 3.1, Figure 3.1. Error at impact of typically 5 m was experienced (10). This is not acceptable.

A somewhat more sophisticated control with 4 states: 1/1 or 1/3 left, 1/1 or 1/3 right, with a high resolution matrix sensor was simulated. Parameter optimization such as varying the medium position amplitude was attempted. However, error at impact was typically 0.7 m on a stationary target, and 4 m on a target moving 10 m/s (10). This 4 state on-off control would be marginally cheaper than a continuous control. Hence 5 state or higher would constitute no saving in production cost. We have not investigated why on-off control is acceptable on a guided bomb but not on the guided grenade. The bomb as known from open literature is subject to less stringent hit accuracy and contains inertial components which improve design flexibility.

3.4.2 Roll, precession and gravity

No simulations have been performed with a rolling grenade. Roll rate less than 20 Hz will have a negligible gyro effect.

The coupling coefficient between roll rate and manoeuvring of the target is difficult to calculate and must be obtained through wind tunnel testing or experiments.

Artillery and mortar pieces have a precession around the velocity vector, initiated at firing and decreasing along the flight path. Aerodynamic studies are required to determine any influence on guidance of the grenade.

A pivoted seeker head will measure angle of attack and compensate for gravity. Alternatively employing a fixed head and estimating the angle of attack α_g due to gravity from the actuator position is only valid on the stationary part of the path.

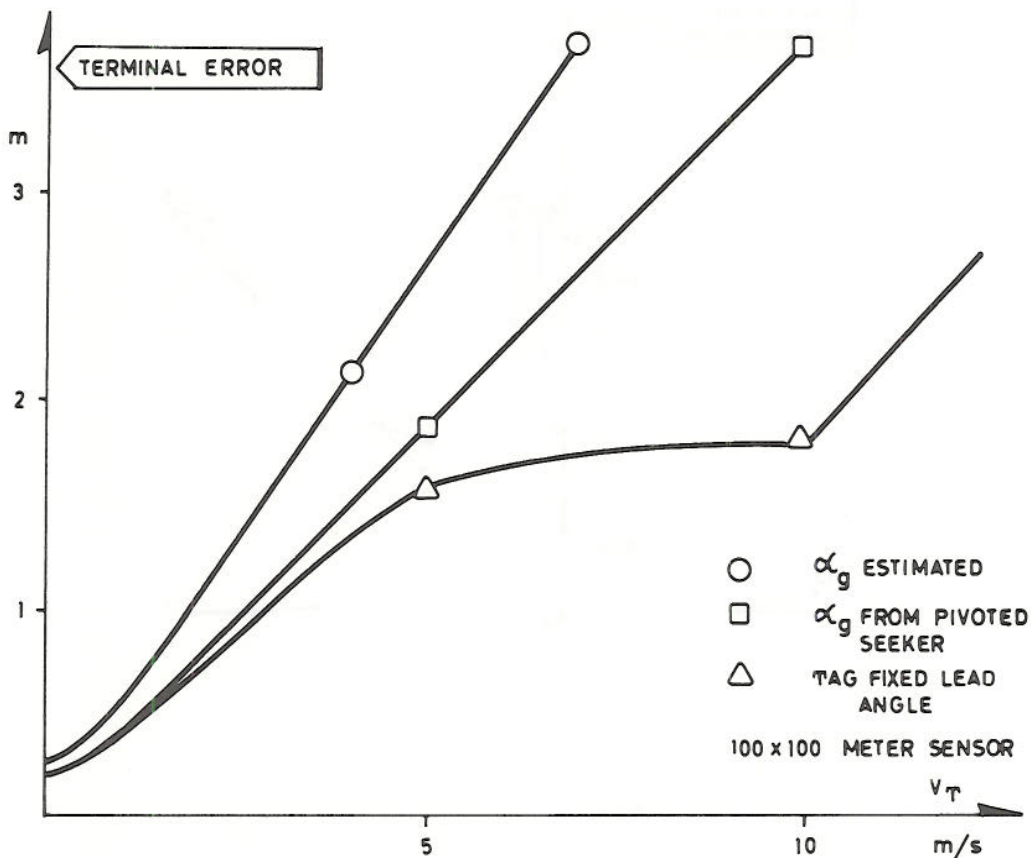


Figure 3.22 Terminal error with target velocity transversal to line of flight

Comparison of simulation results with measured and estimated α_g are shown in Figure 3.22. Aerodynamic studies are recommended to verify the results with estimated α_g .

3.4.3 Moving target

A partial correction for target velocity is "Target Advance Guidance". A fixed lead angle is introduced when the seeker error signal exceeds a specific value on the final path.

Previous measurement of roll rate is used to estimate the correct roll angle to impact. Simulation results for missile terminal errors (21) are multiplied by 1.5 to render equivalent error for a mortar grenade, see Figure 3.22. A fair compensation is achieved for target velocity up to 10 m/s.

Estimating the lead angle according to section 3.3.4 will render compensation for any target velocity within the physical limitations of the grenade. This method was simulated. The compensation network had to be redesigned to make the transfer function overdamped, since the abrupt setting of lead angle makes the grenade more sensitive to underdamped transients than a straight pursuit guidance. The simulations with matrix sensor of resolution 0.15° and high loop gain showed errors of 0.3 m on stationary targets and 2 m on a target moving 8 m/s perpendicular to line of sight. The impact error is mainly due to insufficient sensor resolution. As resolution better than 0.1° is not practical, the solution is reduced loop gain which effectively increases the resolution of grenade angular rate as measured by the sensor, together with a

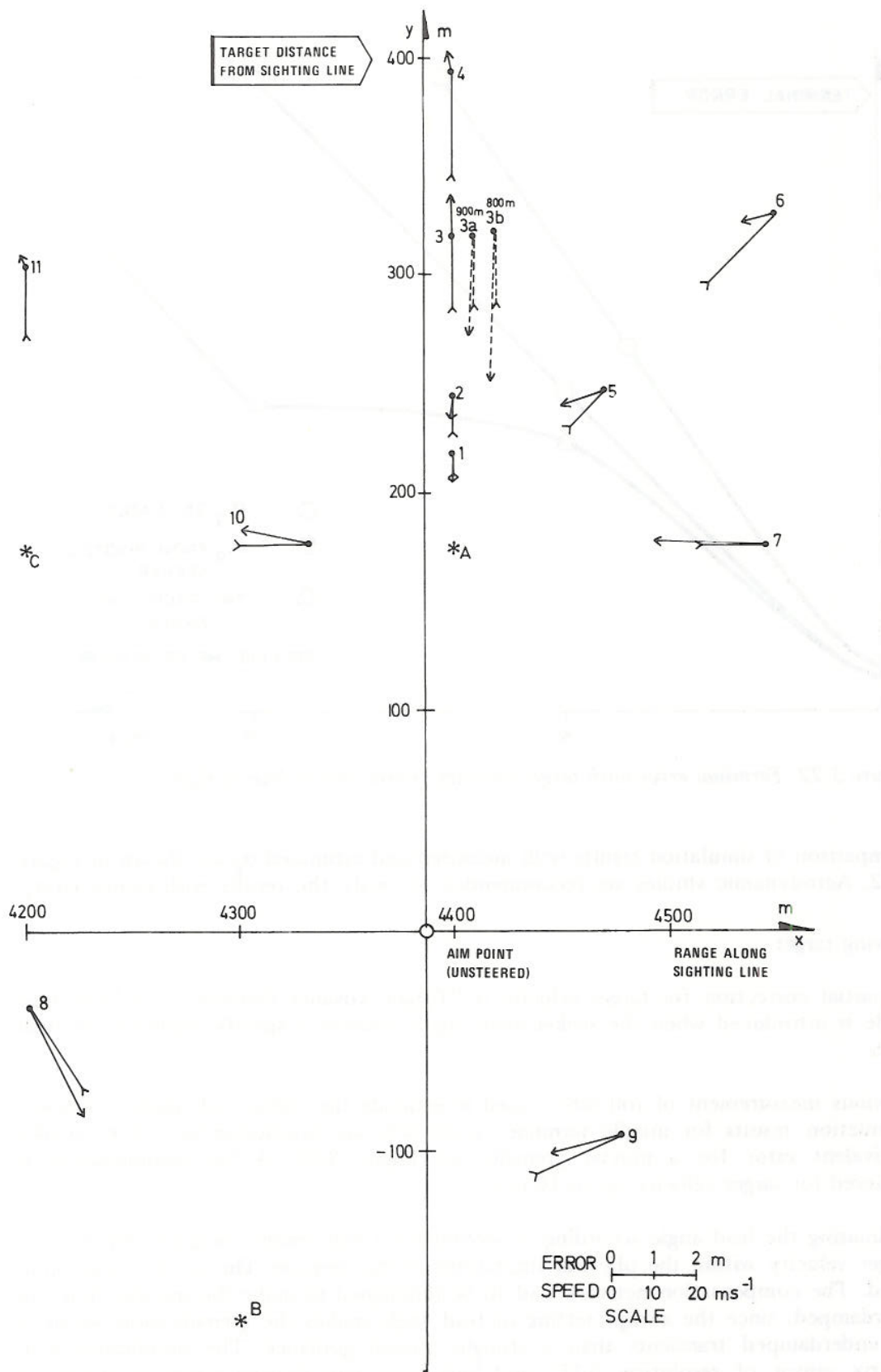


Figure 3.23 Miss distances as a function of target velocity and initial position (11)

- target position at impact
- error direction and magnitude (scale 1 cm = 1.5 m)
- target speed and direction (scale 1 cm = 15 ms⁻¹)
- * initial target positions for the families after a flight time of 25 s, i.e. just prior to "visibility"

parallel gain which compensates for deviation from true pursuit course, see section 3.3.5. This remains to be simulated (10).

The fixed acceleration method of section 3.3.5 has been simulated for a few cases. The results are shown in Figure 3.23. In particular note that the errors are mainly along track the vehicle velocity vector. At a target speed of 8 m/s the error is 0.5 m along track and 0.05 meter across. At 22 m/s the numbers are 1.4 and 0.4 m (11). This is satisfactory on a target vehicle of 6.3×3 m.

4 DESIGN OF A HOMING GRENADE

4.1 Functional description

The small size and extreme launch acceleration of a 107 mm grenade present problems for a practical implementation. The construction of a control unit for side jet, section 3.3.5, has been studied in some detail. Three methods of driving the actuators are:

- a) Pneumatic control of shutters
- b) Gas generators
- c) Torque motors

The first method was investigated for a possible on-off control. Proposals for a system of 8 shutters along the periphery, Figure 4.1, were requested. One vendor (25) was able to offer a solution that will work for grenade roll rate up to 6 Hz with an integral power supply of high pressure air for 10 s operation, at a price of kr 4026,—pr unit for 1000 units. From section 3.4, however, on-off control is too coarse.

Another solution is the rotating cylinder for directional control and an outer cylinder with 2-state pneumatic amplitude control, as shown in Figure 4.2. Conical shield on the nose and cylindrical shield at the air outlet are removed upon target acquisition. The 2-state actuator permits 1/1 and 1/3 of available steering amplitude. This is the design contemplated and simulated for the 4-state on-off control of section 3.4.1.

Gas generators, as used for a similar device (26), are very efficient for a given weight. For the mortar grenade, torque motors offer a simple and reliable solution. 10 s of operation puts moderate demands on the battery.

A design using torque motors to provide continuous control in both direction and amplitude is shown in Figure 4.3. Both the lead angle and fixed acceleration control algorithms can be implemented. This design will be explained in some detail in the following.

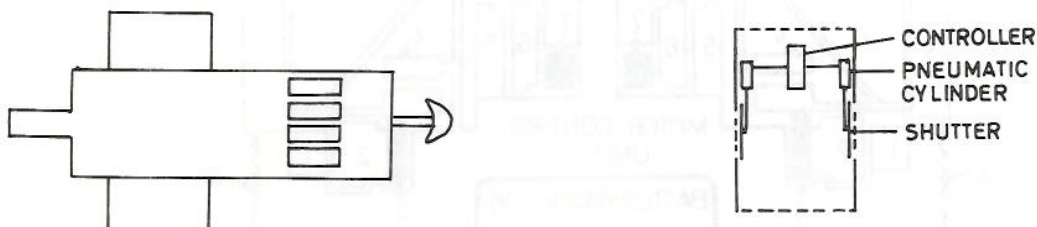


Figure 4.1 Pneumatic actuators, 8 shutters

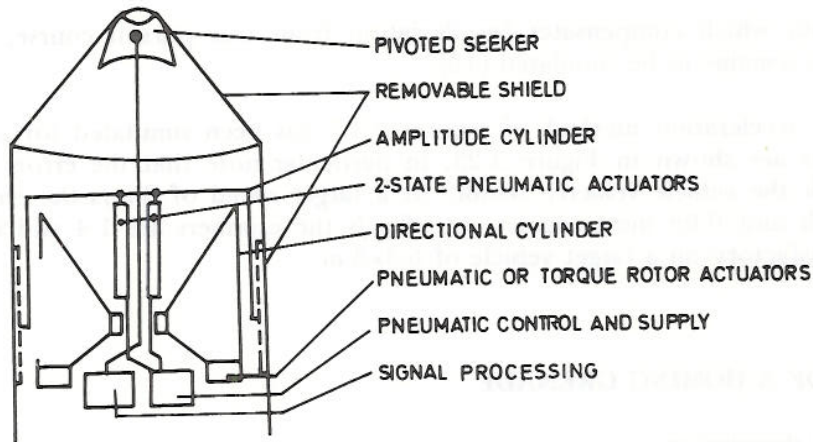


Figure 4.2 Pneumatic control, 2-state amplitude and continuous direction steering

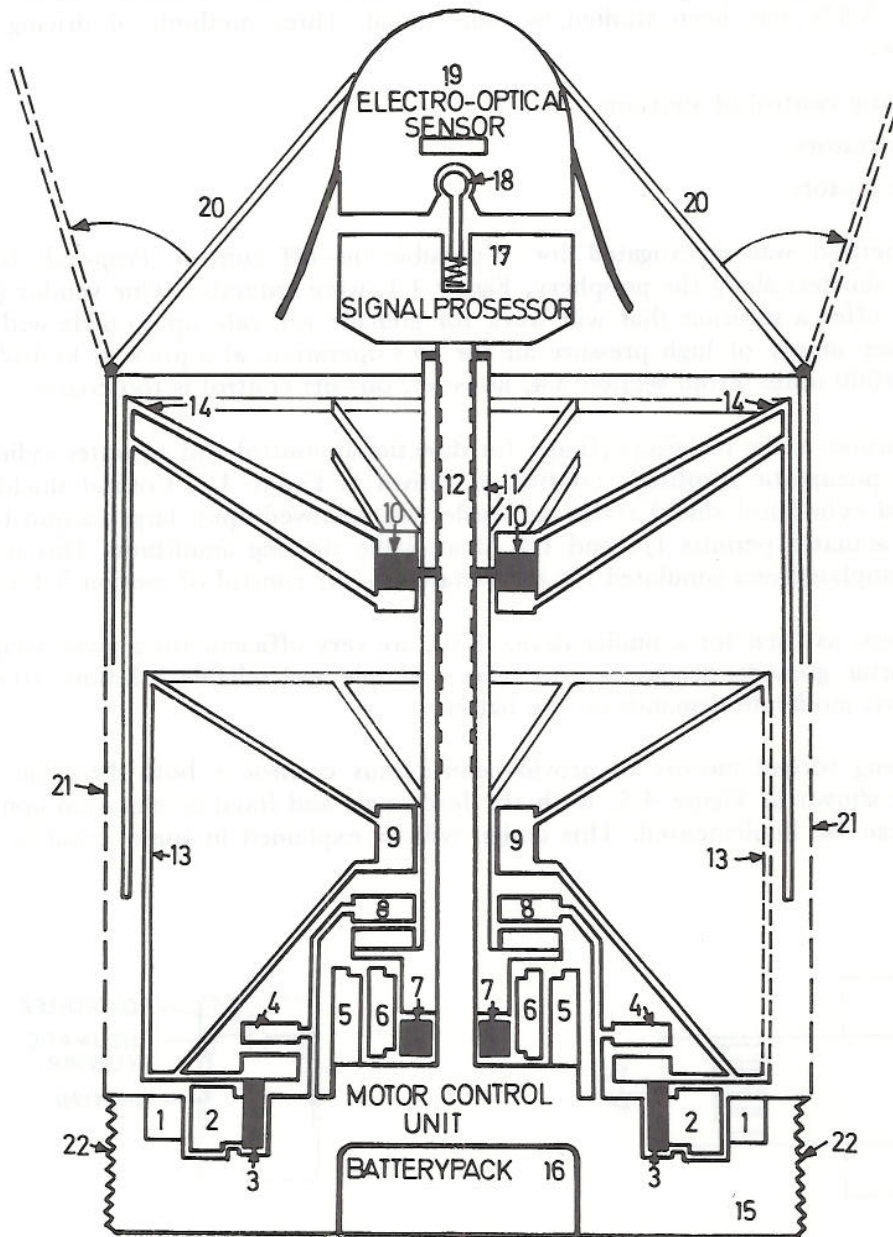


Figure 4.3 Guided grenade seeker and control unit
See parts list, Table 4.1

The outer mantel, 21 in Figure 4.3, is open except for ribs supporting the upper part. The grenade is spin stabilized until target acquisition, when the tail fins and nose shields are unfolded by squibs, causing despin from 100 Hz to 20 Hz in 0.33 s.

The cylinder 13 has a 6x8 cm outlet through the side wall that causes directional control. The actuator is a torque motor 1&2 with potentiometer or code disc 4 for local feedback control. This unit is supported by the bearings 3&9.

Steering amplitude is governed by cylinder 14 supported by bearing 10 and will slide along the ribs in the mantel 21. The seeker head is supported by 12. Inside this tube there will be signal cables.

Tube 12 is threaded on the outside. The outer tube 11 has vertical slots for the stubs of 10 to interact with the threads of 12. The torque motor 5&6 with potentiometer 8 for local feedback control will turn tube 11 causing the cylinder 14 to be hoisted or lowered for control of steering force. The units 6&11 are supported by the ball-bearings 7 and a glide layer at the upper end of the tube 11.

1	STATOR, TORQUE MOTOR 3625-40 (ALT 3629-41 & 3625-80).
2	ROTOR, " " " " FROM MAGTECH INC, USA.
3	SLIDE OR BALL-BEARINGS FOR 2 AND 13.
4	POTENSIOMETER OR CODED DISC MOUNTED ON 2.
5	STATOR, TORQUE MOTOR 1500C-50 (ALT 1937-63).
6	ROTOR, " " " " FROM MAGTECH INC, USA.
7	SLIDE OR BALL-BEARINGS FOR 6 AND 11.
8	POTENSIOMETER OR CODED DISC MOUNTED ON 6.
9	SLIDE BEARING FOR 13.
10	SLIDE BEARING FOR 14.
11	OUTER TUBE WITH VERTICAL SLOTS FOR THE STUBS OF 10.
12	INNER TUBE, CONTAINING SIGNAL CABLES FROM 17 TO 15, THREADED ON THE OUTSIDE TO MATE WITH THE STUBS FROM 10 THROUGH 11. WHEN TURNING 11, 10 WILL BE HOISTED UP OR DOWN.
13	CYLINDER WITH A SIDE WALL HOLE OF 6 x 8 cm FOR DIRECTIONAL CONTROL OF THE SIDE JET.
14	MODULATOR CYLINDER MATED TO 10. WHEN HOISTED, SIDE JET FORCE IS INCREASED.
15	MOTOR CONTROL AMPLIFIERS. LOCAL FEEDBACK FROM 4 AND 8.
16	THERMOELECTRIC BATTERY PACK FROM MARINE APPLIANCES CO LTD GLASGOW (27)
17	ELECTRONIC UNIT, WILL RECEIVE SENSOR SIGNALS AND GENERATE CONTROL SIGNALS.
18	UNIVERSAL JOINT, AND MAGNETOSTRICTIVE SENSOR FROM AMERICAN AEROSPACE CONTROL TO MEASURE ANGLE BETWEEN 17 AND 19.
19	ELECTRO-OPTIC SENSOR IN PIVOTED WEATHER-COCK HEAD.
20	NOSE SHIELDS, TO BE OPENED AT TARGET ACQUISITION.
21	OUTER MANTLE, HIGHLY PERFORATED FOR OUTLET OF THE SIDE JET THROUGH 13.
22	THREADED CONNECTION BETWEEN GUIDANCE HEAD AND THE GRENADE BODY.

Table 4.1 Parts list (the numbers refer to Figure 4.3)

The optical unit 19 is pivoted by 18 in its centre of gravity to permit tilting to both sides but not rotation relative to the support 17 (two degrees of freedom). A skirt on 19 assures alignment with the air stream. Alternatively, a cylinder as used in homing bombs would wind stabilize 19.

A magnetostrictive unit mounted in 19 will measure the angle with the base 17. This angle is equivalent with instantaneous angle of attack α . When fired from the mortar, 19 is supported by 17, whereafter it is pushed forward with the spring 18.

The signal processor is located in 17 to shield the sensor signals from electrical noise from the motor drivers 15. The maximum torque-motor-driver power drain is 200 W. A thermal battery 16 supplying 200 W for 10 s is commercially available (27). To stand the 9000 G, the torque motors shall be so supported that they will rest on the bottom all along the periphery when being launched from the mortar.

It is apparent that a fixed seeker head, if acceptable, would simplify the mechanical design considerably. The nose shield 20 could be shaped sheets of spring steel that are released by lowering cylinder 14, to form a mantel around the seeker head.

One torque motor 5&6 could be replaced by a clutch coupling the other torque motor 1&2 to the amplitude controller shaft 11. A two-way magnetic clutch, Vernitech USA type WMCSC and a geartrain offer some promise of cost reduction, but have not been studied in detail.

4.2 Cost estimate

Research, development including transfer to industry and evaluation have been estimated to 18 Mkr. Image sensor and ECCM hardening will require another 2 Mkr for research and development.

From the design in section 4.1, Figure 4.3, component and assembly cost is calculated in Table 4.2. Based on production of 10 000 units, the estimated grenade cost is kr 9010. Only a few of the items, such as torque motors and thermal battery, are well known at this stage. If 1.9 Mkr for tooling and test equipment is added, a cautious indication of production cost will be kr 9200 per round.

A hybrid-matrix sensor and digital processing for ECCM hardening will add another kr 2800 per round.

A light-weight laser designator is estimated to kr 100 000.

The budget for this program will be:

	No ECCM	With ECCM
Development	18 Mkr	20 Mkr
100 laser designators	10 Mkr	10 Mkr
10 000 grenades	<u>92 Mkr</u>	<u>120 Mkr</u>
Total cost of program	<u>120 Mkr</u>	<u>150 Mkr</u>

Current estimate of user cost for 10 000 guided 107 mm mortar grenades renders:

Without ECCM	12 000 kr per round
With ECCM capability	15 000 kr per round

SUB ASSEMBLIES (FIGURE 4.3)	COST kr	ASSEMBLY & TEST kr	TOTAL kr
SEEKER HEAD			
FRESNEL LENS	50		
QUADRANT SENSOR	600		
4 PREAMPLIFIERS	300		
SIGNAL PROCESSOR	700		
MAGNETOSTRICTIVE ANGLE SENSOR	100		
MECHANICAL PARTS	250		
	2000	1000	3000
DRIVE UNIT			
TORQUE MOTOR (1500C-50) \$95	530		
TORQUE MOTOR (3625-40) \$230	1250		
2 POTENSIOMETERS	320		
2 POWER AMPLIFIERS	300		
VOLTAGE REGULATORS	200		
THERMAL BATTERY, £42	500		
	3100	1200	4300
MECHANICAL PARTS			
DIRECTIONAL CYLINDER	75		
AMPLITUDE CYLINDER	75		
BEARINGS	100		
NOSE SHIELD W/RELEASE MEANS	120		
CASING AND SUPPORT	270		
	640	250	890
GRENADE (PRESENT COST W/IMPACT FUSE)	322		
TAIL FINS WITH SQUIBS	303		
	620	200	820
SUM FOR GUIDED GRENADE			9010

Table 4.2 Grenade cost of production of 10 000 units

4.3 Project organization

Development of a guided grenade should be divided into:

- | | |
|----------|------------------------------------|
| Phase I | Exploratory design and evaluation |
| Phase II | Full scale development and testing |

Phase I would concentrate on:

- Aerodynamic design and testing
- Design of optics, quadrant sensor and preamplifiers
- Construction of control section, with seeker and actuators
- Computer simulation

These items are essential to establish performance and cost of the guided mortar grenade. Design effort a, b, c will provide more realistic parameters for simulations, the result of which interact to improve the grenade construction.

The following may be part of phase I or postponed to phase II:

- e) Hybrid-matrix sensor with digital processing for ECCM
- f) Construction of laser designator
- g) Operational analysis and field trials

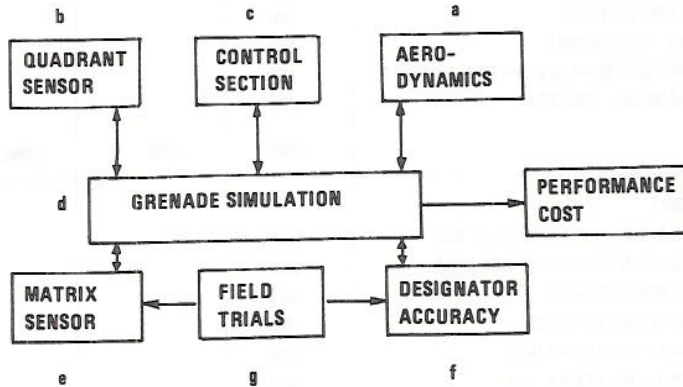


Figure 4.4 Task interaction

Figure 4.4 illustrates how these tasks interact. A shock hardened guided grenade to be launched by a mortar will not be part of phase I. Assuming items e, f and g are part of phase II, development effort is estimated as follows:

	man-year	duration	cost
Phase I	10	1 year	2 Mkr
Phase II, no ECCM	60	2 1/2 year	16 Mkr
Phase II, with ECCM	70	2 1/2 year	18 Mkr

Breakdown in activities are shown in Table 4.3. The project would be organized in subgroups of 2 to 5 persons as indicated. As the design is frozen, project management would become more detailed.

Phase I should be an Army-NDRE project. Phase II would call for industry participation. Thereafter the project responsibility would be transferred to industry, with NDRE activity limited to support and evaluation.

5 CONCLUSION

The feasibility of a semiactive laser guided 107 mm mortar grenade has been investigated.

A design using no inertial components has been simulated. It is expected to have better than 50% hit probability against a vehicle of velocity up to 20 m/s located within a radius of 250 m from the unguided point of impact. Damage probability against a heavy tank will exceed 23% per round launched.

Development and production cost of 10 000 grenades and 100 portable laser designators has been calculated. Divided on 10 000 rounds, estimated user cost is:

Grenade without ECCM	12 000 kr per round
Grenade with ECCM capability	15 000 kr per round

PERSONNEL

PHASE I, DURATION 1 YEAR

SUB-GROUP		NO OF ENGINEERS	
	PROJECT MANAGEMENT	1	
A	AERODYNAMIC DESIGN WIND TUNNEL TESTS MECHANICAL CONSTRUCTION	2	
B	OPTICS, QUADRANT SENSOR, SIGNAL PROCESSING TEST EQUIPMENT	3	
C	ACTUATORS, MOTOR-DRIVER DESIGN	2	
D	COMPUTER SIMULATION, CONTROL THEORY	<u>2</u>	10

PHASE II, DURATION 2 1/2 YEAR

PERSONNEL AS FOR PHASE I WITH THE FOLLOWING ADDITIONS

SUB-GROUP				
A	FIELD TRIALS WITH UNGUIDED GRENADE	2		
B	SEEKER DESIGN, MILITARY SPECIFICATIONS, FIELD TRIALS	2		
C	CONTROL SECTION DESIGN, SHOCK TESTS, FIELD TRIALS	2		
H	GRENADE TEST INSTRUMENTATION FIELD TRIALS WITH GUIDED GRENADE	2		
F	DESIGNATOR DESIGN LASER AND OPTICS 3 TRIPOD <u>1</u>	4		
G	OPERATIONAL ANALYSIS AND EVALUATION WEAPON EFFICIENCY ECCM METHODS	<u>2</u>	<u>14</u>	24
E	ECCM OPTION, ADDITIONS MATRIX SENSOR 1 IMAGE PROCESSING 1 DIGITAL PROCESSOR <u>2</u>	4	<u>4</u>	28

BUDGET

PHASE I	Mkr	Mkr	
10 MAN-YEARS OF 0.17 Mkr	1.7		
OTHER EXPENSES	<u>0.3</u>		
SUM PHASE I	2.0	2	
PHASE II			
24.25 MAN-YEARS OF 0.2 Mkr	12.0		
WIND TUNNEL TESTS, COMPONENTS, WORK-SHOP, INSTRUMENTS, COMPUTER TIME, TRAVEL EXPENSES	<u>4.0</u>		
SUM PHASE II	16.0	<u>16</u>	
SUM DEVELOPMENT			18 Mkr
ADDITIONAL COST OF ECCM OPTION 4.25 MAN-YEARS OF 0.2 Mkr		<u>2</u>	
SUM DEVELOPMENT WITH ECCM OPTION			20 Mkr

Table 4.3 Estimate of development effort

References

- (1) Jacobsen, K O
E Strømsøe — Fragment effect of various types of artillery and mortar ammunition, Intern rapport X-121, Norwegian Defence Research Establishment (1968) Confidential
- (2) Strømsøe, E — Fragment effect of 155 mm howitzer shells against troops in armoured personnel carriers, Teknisk notat VM-203, Norwegian Defence Research Establishment (1975) Confidential
- (3) Kobler, J S
W H Leonard — Assessment of battlefield environments for laser terminal homing systems; Lasers and their military applications, 13 DRG Seminar proc (1973) Confidential
- (4) — Skytetabell for 107 mm bombekaster, TR-6-2, Hærens overkommando (1950)
- (5) Ytreeide, J I — Manøvreringsevne for styrt 105 mm bombekaster prosjektil, Teknisk notat VM-155, Norwegian Defence Research Establishment (1974)
- (6) Høst, S E — Måling av panserkjøretøyers eksponeringstider og panservernskytterses siktefeil, forsøk i Porsanger juni 1974, Notat S-357, Norwegian Defence Research Establishment (1975) Confidential
- (7) Wessel, E G — Eksponeringssannsynlighet for panserkjøretøyer, mulighet for gjeneksponering og målbytte, Notat S-384, Norwegian Defence Research Establishment (1975)
- (8) Toombs, P A B — Guidance of a mortar grenade, Teknisk notat E-571, Norwegian Defence Research Establishment (1973) Confidential
- (9) Toombs, P A B — Guidance system for a homing mortar grenade, Teknisk notat E-617, Norwegian Defence Research Establishment (1974) Confidential
- (10) Ytreeide, J I — Simulation results 1975, to be documented. See (28), (29), (30)
- (11) Toombs, P A B — First order correction of moving-target error of a "tail-chase" homing projectile, Teknisk notat E-760, Norwegian Defence Research Establishment (1975) Confidential
- (12) Toombs, P A B — Laser irradiation detection, Teknisk notat E-537, Norwegian Defence Research Establishment (1973) Confidential

- (13) Lund, T – Laserstyrte våpen – en betenkning om motmidler for forsvar av K&V-anlegg, Teknisk notat E-703, Norwegian Defence Research Establishment (1975) Confidential
- (14) Widenhofer, G H
et al – Laser designators for high accuracy missiles; Lasers and their military applications, 13 DRG Seminar proc (1973) Confidential
- (15) Royce, G – Gun launched laser guided projectiles; Lasers and their military applications, 13 DRG Seminar proc (1973) Confidential
- (16) Andersen, K – Slutfasstyrd og slutfaskorrigerad artilleriammunition – hybrider av konventionelt artilleri och robotar, Tidsskr för Kustartilleriet 33, 145-52 (1975)
- (17) Regan, F J
J Smith – The aeroballistics of a terminally corrected spinning projectile (TCSP), Paper 74-796, AIAA Mechanics and Control of Flight Conference, 5-9 Aug 74 (1974)
- (18) Bugge-Asperheim, P – Styring av bombekastergranat, noen enkle beregninger, Teknisk notat E-658, Norwegian Defence Research Establishment (1974) Confidential
- (19) Sokolnikoff, I S – Mathematics of physics and modern engineering, ch 2.6, McGraw-Hill Book Co, New York (1966)
- (20) Locke, A S – Principles of guided missile design, ch 12, D Van Nostrand Co, New Jersey (1955)
- (21) Ytreeide, J I – Krumbane panservernrakett med multielement detektor, Teknisk notat VM-167, Norwegian Defence Research Establishment (1974) Restricted
- (22) Puckett, A
S Ramo – Guided missile engineering, McGraw-Hill Book Co, New York (1959)
- (23) Chestnut, H
R W Mayer – Servomechanisms and regulating systems, 1, ch 8.4, J Wiley & Sons, New York (1959)
- (24) Bugge-Asperheim, P – Styring av granat mot bevegelig mål, H7021/75/FFIE, Norwegian Defence Research Establishment (1975) Confidential
- (25) – Pneumatisk syklusstyring av sylindere, Letter of 16 Dec 74 to NDRE/E from P D Wærner A/S, Oslo, for Herion-Werke, Stuttgart, DBR
- (26) Robinson, C A – Wings to boost guided projectile range, Aviat Week Space Technol 103, 15 (1975)

- (27) Young, W R — Letter of 5 Sep 75 to NDRE/E from Mine Safety Appliances Co Ltd, Queenslie Industrial Estate, Glasgow
- (28) Ytreeide, J I — Aerodynamikk for 107 mm Bk-prosjektil som styres med luftstrømsavbøyning, Teknisk notat VM-220, Norwegian Defence Research Establishment (1975) Confidential (In preparation)
- (29) Ytreeide, J I — Modell av sluttstyring for antipanserprosjektiler, Teknisk notat VM-227, Norwegian Defence Research Establishment (1976) Confidential (In preparation)
- (30) Ytreeide, J I — Simulering av styrt 107 mm bombekasterprosjektil, Teknisk notat VM-228, Norwegian Defence Research Establishment (1976) Confidential (In preparation)